

Capturing and analyzing pattern diversity: an example using the melanistic spotted patterns of leopard geckos (#59417)

1

First submission

Guidance from your Editor

Please submit by **17 Apr 2021** for the benefit of the authors (and your \$200 publishing discount) .



Structure and Criteria

Please read the 'Structure and Criteria' page for general guidance.



Custom checks

Make sure you include the custom checks shown below, in your review.



Raw data check

Review the raw data.



Image check

Check that figures and images have not been inappropriately manipulated.

Privacy reminder: If uploading an annotated PDF, remove identifiable information to remain anonymous.

Files

Download and review all files from the [materials page](#).

12 Figure file(s)

1 Table file(s)

2 Other file(s)

! Custom checks

Vertebrate animal usage checks



Have you checked the authors [ethical approval statement](#)?



Were the experiments necessary and ethical?



Have you checked our [animal research policies](#)?



Structure and Criteria

Structure your review

The review form is divided into 5 sections. Please consider these when composing your review:

1. BASIC REPORTING
2. EXPERIMENTAL DESIGN
3. VALIDITY OF THE FINDINGS
4. General comments
5. Confidential notes to the editor

You can also annotate this PDF and upload it as part of your review

When ready [submit online](#).

Editorial Criteria

Use these criteria points to structure your review. The full detailed editorial criteria is on your [guidance page](#).

BASIC REPORTING

- Clear, unambiguous, professional English language used throughout.
- Intro & background to show context. Literature well referenced & relevant.
- Structure conforms to [Peerj standards](#), discipline norm, or improved for clarity.
- Figures are relevant, high quality, well labelled & described.
- Raw data supplied (see [Peerj policy](#)).

EXPERIMENTAL DESIGN

- Original primary research within [Scope of the journal](#).
- Research question well defined, relevant & meaningful. It is stated how the research fills an identified knowledge gap.
- Rigorous investigation performed to a high technical & ethical standard.
- Methods described with sufficient detail & information to replicate.

VALIDITY OF THE FINDINGS

- Impact and novelty not assessed. Negative/inconclusive results accepted. *Meaningful* replication encouraged where rationale & benefit to literature is clearly stated.
- All underlying data have been provided; they are robust, statistically sound, & controlled.
- Speculation is welcome, but should be identified as such.
- Conclusions are well stated, linked to original research question & limited to supporting results.



The best reviewers use these techniques

Tip

Example

Support criticisms with evidence from the text or from other sources

Smith et al (J of Methodology, 2005, V3, pp 123) have shown that the analysis you use in Lines 241-250 is not the most appropriate for this situation. Please explain why you used this method.

Give specific suggestions on how to improve the manuscript

Your introduction needs more detail. I suggest that you improve the description at lines 57- 86 to provide more justification for your study (specifically, you should expand upon the knowledge gap being filled).

Comment on language and grammar issues

The English language should be improved to ensure that an international audience can clearly understand your text. Some examples where the language could be improved include lines 23, 77, 121, 128 - the current phrasing makes comprehension difficult. I suggest you have a colleague who is proficient in English and familiar with the subject matter review your manuscript, or contact a professional editing service.

Organize by importance of the issues, and number your points

- 1. Your most important issue*
- 2. The next most important item*
- 3. ...*
- 4. The least important points*

Please provide constructive criticism, and avoid personal opinions

I thank you for providing the raw data, however your supplemental files need more descriptive metadata identifiers to be useful to future readers. Although your results are compelling, the data analysis should be improved in the following ways: AA, BB, CC

Comment on strengths (as well as weaknesses) of the manuscript

I commend the authors for their extensive data set, compiled over many years of detailed fieldwork. In addition, the manuscript is clearly written in professional, unambiguous language. If there is a weakness, it is in the statistical analysis (as I have noted above) which should be improved upon before Acceptance.

Capturing and analyzing pattern diversity: an example using the melanistic spotted patterns of leopard geckos

Tilman Glimm ^{Corresp., 1}, Maria Kiskowski ², Nickolas Moreno ³, Ylenia Chiari ³

¹ Department of Mathematics, Western Washington University, Bellingham, Washington, United States

² Department of Mathematics and Statistics, University of South Alabama, Mobile, Alabama, United States

³ Department of Biology, George Mason University, Fairfax, Virginia, United States

Corresponding Author: Tilman Glimm

Email address: glimmt@wwu.edu

Animal color patterns are widely studied in ecology, evolution, and through mathematical modeling. Patterns may vary among distinct body parts such as the head, trunk or tail. As large amounts of photographic data is becoming more easily available, there is a growing need for general quantitative methods for capturing and analyzing the full complexity and details of pattern variation. Detailed information on variation in color pattern elements is necessary to understand how patterns are produced and established during development, and which evolutionary forces may constrain such a variation. Here, we develop an approach to capture and analyze variation in melanistic color pattern elements in leopard geckos. We use this data to study the variation among different body parts of leopard geckos and to draw inferences about their development. We compare patterns using 14 different indices such as the ratio of melanistic versus total area, the ellipticity of spots, and the size of spots and use these to define a composite distance between two patterns. Pattern presence/absence among the different body parts indicates a clear pathway of pattern establishment from the head to the back legs. Together with weak within-individual correlation between leg patterns and main body patterns, this suggests that pattern establishment in the head and tail may be independent from the rest of the body. We found that patterns vary greatest in size and density of the spots among body parts and individuals, but little in their average shapes. We also found a correlation between the melanistic patterns of the two front legs, as well as the two back legs, and also between the head, tail and trunk, especially for the density and size of the spots, but not their shape or inter-spot distance. Our data collection and analysis approach can be applied to other organisms to study variation in color patterns between body parts and to address questions on pattern formation and establishment in animals.

1
2 **Capturing and analyzing pattern diversity: an example using the**
3 **melanistic spotted patterns of leopard geckos**

4
5
6 Tilmann Glimm¹, Maria Kiskowski², Nickolas Moreno³, Ylenia Chiari³

7
8 ¹*Western Washington University, Department of Mathematics, Bellingham, WA 98229, USA*

9 ²*University of South Alabama, Department of Mathematics and Statistics, Mobile, AL 36688,*
10 *USA*

11 ³*George Mason University, Department of Biology, Fairfax, VA 20110, USA*

12
13 Corresponding Author:

14 Tilmann Glimm

15 Western Washington University

16 Department of Mathematics

17 516 High Street, Bellingham, WA 98226

18 Email address: glimmt@wwu.edu

19
20 **Abstract**

21 Animal color patterns are widely studied in ecology, evolution, and through mathematical
22 modeling. Patterns may vary among distinct body parts such as the head, trunk or tail. As large
23 amounts of photographic data is becoming more easily available, there is a growing need for
24 general quantitative methods for capturing and analyzing the full complexity and details of
25 pattern variation. Detailed information on variation in color pattern elements is necessary to
26 understand how patterns are produced and established during development, and which
27 evolutionary forces may constrain such a variation. Here, we develop an approach to capture
28 and analyze variation in melanistic color pattern elements in leopard geckos. We use this data
29 to study the variation among different body parts of leopard geckos and to draw inferences
30 about their development. We compare patterns using 14 different indices such as the ratio of
31 melanistic versus total area, the ellipticity of spots, and the size of spots and use these to define
32 a composite distance between two patterns. Pattern presence/absence among the different
33 body parts indicates a clear pathway of pattern establishment from the head to the back legs.
34 Together with weak within-individual correlation between leg patterns and main body patterns,
35 this suggests that pattern establishment in the head and tail may be independent from the rest
36 of the body. We found that patterns vary greatest in size and density of the spots among body
37 parts and individuals, but little in their average shapes. We also found a correlation between the
38 melanistic patterns of the two front legs, as well as the two back legs, and also between the
39 head, tail and trunk, especially for the density and size of the spots, but not their shape or inter-
40 spot distance. Our data collection and analysis approach can be applied to other organisms to
41 study variation in color patterns between body parts and to address questions on pattern
42 formation and establishment in animals.

43

44 Introduction

45 Animal color patterns vary within and among individuals, including variation among distinct body
46 parts such as the head, trunk, tail, wings, or ventral or dorsal sides, possibly in response to
47 different selection pressures (Caro, 2005; Forsman et al., 2008; Allen et al., 2020). Color
48 patterns may differ in qualitatively obvious ways, such as stripes on the tail and spots on other
49 parts of the body, or in more subtle ways, such as spots of different density or sizes (e.g., Figure
50 1). Variation in color pattern is considered a classical example of an adaptive trait, as it is often
51 involved in communication among conspecifics, intrasexual competition, and antipredator
52 functions (Caro, 2005; Gomez et al. 2007, Tibbetts and Dale, 2004, Solan et al. 2019).

53 Although color patterns have been studied extensively because they are involved in
54 many functions essential to the survival and reproduction of organisms, describing and
55 quantifying pattern variation in a multivariate manner is still challenging. Color patterns are
56 generally described in terms of macroscopic differences, such as spots, stripes or labyrinthine
57 organization (e.g., Miyazava et al. 2010, Allen et al. 2020, Kuriyama et al. 2020), with pattern
58 variation for the same pattern type often quantified using landmarks obtained on homologous
59 pattern features (e.g., van Belleghem et al 2018, Bainbridge et al. 2020, Prinsloo et al. 2020) or
60 by focusing on differences in pattern elements, coarsely defined in terms of relative size and
61 position (e.g., van den Berg et al. 2020 and references therein). However, complex patterns with
62 high degree of dissimilarity within and among individuals in terms of shape, clustering, size and
63 position of the pattern elements may require the development of new methods to finely capture
64 these differences (see for example Lee et al. 2018 and references therein) This is particularly
65 pertinent if the shape and density are irregular and do not fit within specific pattern categories,
66 such as stripes or spots (Solan et al., 2019; Troscianko et al., 2017; Lee et al., 2018; Miyazawa
67 et al. 2010; McGuirl et al., 2020; Allen et al., 2020).

68 Color pattern can be studied using pattern recognition, which broadly speaking deals
69 with classification of image patterns through extraction of significant features (Zerdoumi et al.,
70 2018). Methods in this area generally consist of machine learning techniques, that is, the
71 prediction systems based on an existing data set. For example, this could entail classification of
72 skin patterns based on a large training data set of skin pattern images. While this approach is
73 certainly viable for synthetic data, i.e. computer-generated patterns (McGuirl et al, 2020), where
74 data with thousands of patterns can be amassed easily, this approach may not be feasible for
75 actual images of live animals, where the process of image acquisition is laborious and time
76 consuming. In addition, the use of machine learning techniques would not necessarily provide
77 qualitative insights into what would make two or more patterns similar or different (Domingos,
78 2012; Zerdoumi et al., 2018), therefore impeding investigation of what elements of the pattern
79 for example may be more or less variable, constrained or under selection.

80 In this article, we address the problem of describing and quantifying variation in
81 melanistic color patterns in live geckos via computing fourteen different indices, such as the
82 fraction of dark areas to light ones, or the mean size, number and shape of pattern features.
83 Each of these different indices captures only one aspect of the pattern, but collectively, they
84 yield a comprehensive characterization of the pattern itself. Thus, each pattern of the seven
85 body parts studied for each individual corresponds to a point in an abstract 14-dimensional
86 space (here called “pattern space” or “phenotype space”). Our approach is similar to that of Lee

87 et al. (2018) who used 11 indices to characterize giraffe coat patterns and Miyazawa et al.
88 (2010), who used two indices to describe salmonid fish skin patterns. In contrast to those
89 papers, however, we not only compare single indices between individuals and among
90 individuals, but also consider different ways to measure the overall similarity of two patterns
91 based on their distance in pattern space, taking into account biological information in the data
92 set. In this, our approach is therefore innovative. Arguably, there is no canonical distance
93 function on this multidimensional space to measure overall similarity of patterns, and so we
94 employ two different notions of a metric, both weighted Euclidean distances. These two
95 distances differ in the type of biological information that they may provide. The first distance, the
96 standard Mahalanobis distance, essentially weights each principal component by the inverse of
97 its variance (Mahalanobis, 1927; Krzanowski, 2000). This standard metric weighs all data points
98 equally and thus does not take into account any inherent structure of the data set, as for
99 example any developmental relationship among body parts. The second distance that we
100 selected is instead a measure that weights differences in patterns by the influence of random
101 noise in the developmental process. We call this distance the “Developmental Noise distance”.
102 In it, differences in indices for which developmental noise has a small contribution are weighted
103 heavier than differences in indices for which it has a larger contribution. The use of these two
104 distance measures therefore not only permits to quantitatively describe and statistically test
105 pattern variation, but also to help understanding the developmental sources - genotypic,
106 environmental, or stochastic - of this variation.

107 We apply our new approach to capture pattern data and our pattern distance measures
108 to investigate the variation of melanistic skin patterns among distinct body parts for 25 leopard
109 geckos (*Eublepharis macularius*) (Figures 1 and 2 and Table 1). We use these data to analyze
110 different pattern indices and calculate their correlation to infer the order of pattern formation and
111 establishment across the body and to characterize pattern variation on the different body parts
112 within and among geckos. Finally, by comparing the within-individual left-right variation in leg
113 patterns, which is likely due to developmental noise, to the between-individual variation, which is
114 due to genetic and environmental differences in addition to developmental noise, we quantify
115 the influence of developmental noise on pattern variation for the leopard gecko.

116 Among vertebrates, lizards have often been used as ideal models to study the evolution
117 of color and color pattern in relationship to other ecological, biological, and behavioral traits
118 (e.g., Olsson et al., 2013; Pérez I de Lanuza and Font, 2016; Murali et al., 2018; Allen et al.,
119 2020). Specifically, the leopard gecko is an ideal organism on which to study pattern
120 development (e.g., Chang et al., 2009). This species is commonly bred in captivity to obtain
121 distinct colors and color patterns, a major advantage when trying to unveil the mechanisms
122 producing variation at these traits (Cieslak et al. 2011). Furthermore, our previous work on color
123 patterns on the head of this species (Kiskowski et al., 2019) suggests that developmental noise
124 may be an important contributor to its variation.

125 This work therefore not only proposes a novel approach to analyze similarities in pattern
126 space within and among individuals, but also contributes to our understanding of melanistic
127 pattern formation and establishment in the leopard gecko. The data capture and analysis
128 methods presented here can also be applied to study variation in color pattern elements for
129 developmental, ecological and evolutionary purposes in other organisms. Furthermore, our
130 previous work used mathematical modeling of the process of skin pattern formation to elucidate

131 the influence of developmental noise on patterning (Kiskowski et al., 2019). Many different other
132 mathematical models for skin patterning have been proposed (e.g. Murray, 2002; Cruywagen et
133 al., 1992; Painter, 2001; Cooper et al., 2018; Kondo et al., 2009). In this context, developmental
134 noise can be modeled for example by using random initial conditions for the equations
135 governing pattern formation. Because of this randomness, the resulting pattern is not
136 deterministic, but rather a certain range of possible patterns - all depending on randomization of
137 these initial conditions - may be generated with an associated probability density function. This
138 range can be thought of as a set of points in the 14-dimensional pattern space provided by the
139 measures used in the current work. This approach and the empirical data can then be used to
140 assess the validity of the models, and thus in turn biological insights (see McGuirl et al. 2020 for
141 an example) into the patterning process.

142

143 **Materials & Methods**

144 *Ethical statement:*

145 All experiments were carried out in accordance with George Mason University animal use
146 (IACUC) protocol # 1430668.

147

148

149 **Geckos and Photographs**

150 For this study we used a total of 25 live adults of *Eublepharis macularius*, the leopard gecko,
151 giving a total of 132 patterns on various body parts. 20 geckos had an overall "normal" pattern
152 morphotype (melanistic - black - spots on a yellowish/brownish background), while five geckos
153 had a "lemon frost" morphotype with melanistic patterns (Szydłowski et al. 2020, Guo et al.
154 2020; Figure A1 in the Appendix for full body images of all geckos, Table 1 and Supplementary
155 Material for details on the origin of the geckos).

156 We photographed the geckos one at the time by placing each one of them on a smooth
157 surface covered with colored paper (RGB=[100,60,65], Figure 1) chosen to contrast well with
158 the full set of geckos in at least one color channel) (Figure A1 in the Appendix). Perpendicular
159 reference lines were printed on the colored paper to ensure placement of the gecko in the same
160 position across picture sets. For each gecko, we obtained four picture sets to measure the error
161 associated with the data capture (See Supplementary Material for further details).

162

163

164

165 **Image Analysis**

166 The melanistic spotted patterns were studied on the head, four limbs, dorsal trunk, and tail of
167 each of the 25 geckos. There were thus $25 \times 7 = 175$ separate body parts analyzed in this work
168 (Figure 3). Not all these body parts showed melanistic spotted skin patterns and only twelve of

169 the geckos had qualifying spotted patterns on all seven body parts (Table 1; see details below
170 for how qualifying patterns were recognized).

171 For our analyses, each of the seven regions for each gecko was isolated by automated
172 removal of background pixels from the images where possible and additionally by hand using
173 the GIMP photo editing tool (Figure 3). When cutting the regions, we worked along the natural
174 boundary of the body and had defined rules for the edges of the body region (e.g., the trunk was
175 separated from the head by a straight line segment connecting the two most anterior points
176 where each front legs met the main body, and the legs were separated from the body using a
177 straight line segment perpendicular to the limb that was the most proximal line segment that
178 could be drawn without including any portion of the trunk. See Figure A3 for more details). For
179 each of the 700 images (25 geckos, 7 body parts, 4 independent photos of each), we identified
180 and isolated the spotted melanistic pattern as a simple binary pattern of black pixels on a white
181 background (i.e., in every image, each pixel has either value of 1 = black or 0 = white). Using
182 criteria to help in isolating the melanistic spotted pattern amongst other patterns of the skin and
183 background noise of the image, a threshold was applied to each of the regions to define the
184 binary pattern of black spots on a white background (see below for details and Table 2). A spot
185 identification algorithm was applied for each type of body pattern to identify spots. A final image
186 processing step with Matlab removed stray pixels, filled in holes, and smoothed the contour of
187 the spots to generate the final spot patterns used for measuring the pattern statistics. The
188 Matlab code for these scripts are available in the Supplementary Material (after acceptance of
189 the manuscript for publication).

190

191

192 **Limb, Trunk, Head, and Tail Spot Identification Algorithms**

193 Due to morphological differences in the four body parts, the algorithms used to determine the
194 melanistic pattern from the photographic images varied for each body part, but was otherwise
195 applied the same way to every gecko image for uniformity and consistency. In a preliminary step
196 that was completed by trial and error and evaluated by eye, all rules for the algorithm (for
197 example, which color channel to use, whether the lighting across the images would be adjusted,
198 and the threshold darkness criterion for which a pixel would be identified as melanistic or not)
199 were chosen for each body part for a good fit between paucity (to minimize the number of
200 criteria and minimize differences between the four algorithms) and robust ability (as determined
201 by eye) to capture the melanistic patterning for the greatest number of gecko images.

202 All of the differences between the four algorithms are summarized in the Supplementary
203 Material. See Supplementary Material for images of all 7 body parts and binarized images for 25
204 geckos (times 4 repeated measurements); also see Figure A2 in the Appendix for a
205 representative example of the binarized images for one body part for one gecko.

206

207 **Image Length Scale:** For each image, the length scaling factor (length per pixel) was computed
208 via determining the number of pixels for one centimeter using the imaging software GIMP. This
209 was used in converting values measured in pixels to lengths, see Table 3.

210

211 **Application of a Threshold to Define Spots**

212 Each pixel of an image has an R, a G and a B value, which are integers that each range from 0
213 to 255. We used the green channel G as a measure of the intensity of a spot (see Table 2).
214 Threshold intensities for determining whether a pixel in an image was dark enough to be a pixel
215 within a melanistic spot was based on the average intensity μ and the standard deviation σ of the
216 intensity within the region. For the legs, trunk and tail, a threshold of $\mu - 0.85\sigma$ was determined
217 by eye to best capture the melanistic pattern across the entire set of geckos. For the head,
218 which had a larger fractional area of melanistic spots, a threshold $\mu - 0.5\sigma$ was determined to
219 identify the set of melanistic spot pixels best. A high fraction of melanistic **area** relative to total
220 skin area (combined with exceptionally dark spots) would decrease the average intensity to
221 values that were too low to identify more lightly colored spots so a minimum was applied that
222 the threshold for the value of a pixel would be at least 60 out of 255. Pixels with values this low
223 were invariably likely to be melanistic. A maximal threshold of 108 out of 255 was applied to the
224 trunk since a very low fractional melanistic area could cause the average intensity to be too
225 large for good spot detection; however, higher threshold values were frequently appropriate for
226 other body parts (for the legs for example) so no maximal threshold was applied for parts other
227 than the trunk.

228
229

230 **Final Pattern Processing**

231 The application of the threshold identified a set of pixels that are darker than the threshold value
232 for each evaluated image. This set of pixels included stray pixels as well as larger contiguous
233 areas of pixels that were likely to be pigmented spots. A minimum spot size of 350 pixels (~ 0.5
234 mm^2) was required for the spot to be qualified as such in this work. This number was
235 determined by visual inspection to remove stray pixels and very small dark artifacts. Although
236 the size of pigmented regions varied (especially the size of these regions could be very large on
237 the head and the trunk), none of the pigmented areas that should be identified as spots were
238 smaller than about 750 pixels in total area, so the minimum spot size was chosen to be smaller
239 than the pigmented areas the algorithm needed to identify but larger than most artifacts.

240 In the last processing steps, any holes within pigmented regions (see Supplementary
241 Material Figure S1, Panel F) were filled, and the contour of the spots was smoothed using
242 successive dilations and erosions (this removes small scale granular effects at the edges of
243 spots without changing the shape of the spot). See the Supplementary Material for details.

244

245 **Final Pattern Classification**

246 For both the limb and trunk patterns, the spotted pigmented pattern would occasionally be very
247 faint and barely present or not present at all. To distinguish among these, an image was
248 classified as a patterned only if there were at least four interior spots for limb patterns and at
249 least six interior spots for the trunk and tail. The head was invariably well-patterned, with at least
250 26 spots found on the heads of all the geckos, so no minimum was applied.

251
252

253 Description of indices

254 For each of the 25 geckos, we excluded images without patterns as determined by the algorithm
 255 described above (Tables 1 and 2) giving a total of 132 qualifying patterns (14-16 patterns for
 256 each of the 4 legs, 23 trunk patterns, 25 head patterns and 25 tail patterns). For each such
 257 qualifying combination of body parts and gecko, we used Matlab to calculate the 14 indices
 258 summarized in Table 3. The value of each index is the average of the 4 independent
 259 measurements, giving a total of $132 \times 4 = 528$ images that were analyzed. For an assessment of
 260 the measurement error, see below and the Supplementary Material.
 261

262

263 Definition of distances on pattern space: Mahalanobis and 264 Developmental Noise distances

265 Each qualifying pattern (one of 7 body parts of one of 25 geckos) is described by the 14 indices
 266 in Table 3. Thus we can think of a pattern as a point $\vec{x} = (x_1, \dots, x_{14})^T$ in a 14-dimensional pattern
 267 space. (The superscript "T" denotes the transpose). To quantify the similarity of two patterns, we
 268 measure the distance between two points in this pattern space. We consider two different
 269 definitions of a distance (metric) on pattern space. Let $\vec{x} = (x_1, \dots, x_{14})^T$ and $\vec{y} = (y_1, \dots, y_{14})^T$
 270 denote two points. The first distance we consider is the standard Mahalanobis distance given by

$$271 \quad d_N(\vec{x}, \vec{y}) = \sqrt{(\vec{x} - \vec{y})^T S^{-1} (\vec{x} - \vec{y})}.$$

272 Here S is the covariance matrix of the complete data set. One can think of the Mahalanobis
 273 distance as the Euclidean distance computed after transforming the data to principal
 274 components and normalizing each principal component (Krzanowski, 2000). The advantage of
 275 this method over the Euclidean distance on the untransformed pattern space is that the principal
 276 components are uncorrelated, and so the Mahalanobis distance is not skewed by correlations
 277 between the different indices. It is generally regarded as an appropriate generic choice for a
 278 statistical distance in sample spaces with differential variances and correlations (Krzanowski,
 279 2000). As a generic choice however, the Mahalanobis distance does not take into account any
 280 specific information from the particular structure of our data set. In the case at hand, the data
 281 points can be grouped by animal, by body part, or for instance by pairs of front legs or back legs
 282 of the same animal. In general, differences among patterns can be attributed to differences in
 283 the genotype, the environment experienced, and developmental noise. The differences among
 284 patterns within the pairs of data points describing the front legs or the back legs of the same
 285 animal are likely primarily the result of developmental noise, as opposed to two different
 286 genotypes or different environmental conditions. Data obtained from the legs allow then to
 287 separate the influence of developmental noise from genetic and environmental factors. We take
 288 this into account and define a second metric called "Developmental Noise metric", defined as a
 289 weighted Euclidean metric:

$$290 \quad d_D(\vec{x}, \vec{y}) = \sqrt{\sum_{i=1}^{14} w_i (x_i - y_i)^2},$$

291 where the weights w_i , $i = 1, \dots, 14$ are defined via the standard deviation of the two front leg
292 patterns of each gecko. More specifically, for the index i (with $1 \leq i \leq 14$), let S_i^n denote the
293 variance of the indices of the two front leg patterns of the n th gecko (we only included geckos
294 that have patterns on all four legs; see Table 1). Then we define the weight w_i as the inverse of
295 the mean of the variances S_i^n , i.e.

$$296 \quad w_i = \frac{1}{\text{mean}(S_i^n)} \quad (1 \leq i \leq 14),$$

297 where the mean is taken over all geckos who have patterns on front legs. Note that this distance
298 function is scale invariant, i.e. independent of the units used for the different indices. The reason
299 for using these weights is that the mean variance between the two front legs is a rough measure
300 for the importance of noise in the establishment of the pattern; thus effectively the fewer
301 influence noise has on a measurement, the more weight it is given in the computation of the
302 distance between patterns. While this distance takes into account the special structure of the
303 data set, its computation is based only on a subset of the data, namely leg patterns of those
304 geckos that have patterned front legs. This is in contrast to the standard Mahalanobis metric,
305 which ignores the special structure, but is based on all data points. It is a priori not clear which
306 of these distances is more appropriate, and for this reason we use both in the following
307 analyses. In fact, we found that in general, the results for these two metrics agree qualitatively,
308 giving added confidence in our results (see Results section). Many other reasonable concepts
309 of distances on pattern space are possible. Results are reported in all cases for the *squares* of
310 the distances.
311

312 Quantification of measurement error

313 We took four independent photos of each body part, where the animal was picked up and
314 rearranged for each repetition so that the four measurements would be independent. A
315 measurement error was introduced by slight differences in the rotation and placement,
316 especially for the limbs and tail. To quantify the measurement error, we took two approaches: in
317 the first, we compared the mean distances in pattern space between the different
318 measurements to the mean between-individual distances of the same body part. The second
319 consisted of a two-way ANOVA test for the front legs and the back legs, where the two factors
320 are “sides” (S , fixed) and “individuals” (I , random). For more details, see the “Results” section
321 below.

322

323 Statistical Analysis and Software

324 Images of various body parts were extracted via automated removal of background pixels and
325 consequent manual selection from photos of the geckos with the image editor GIMP. All
326 computations for image analysis and statistical analysis were performed with Matlab. The
327 computations of statistical significance of results (p -values) were performed either with standard

328 statistical tests as implemented in Matlab where indicated, or via nonparametric permutation
329 tests (see the Appendix for details on the procedure). The Matlab code is available in the
330 Supplementary Material (after acceptance of the manuscript for publication).

331

332

333 Results

334 Patterning

335 Table 1 shows that not all geckos had melanistic patterns that were identified on all body parts.
336 In some cases there was no visible spot pattern by eye as well, in some cases the pigmented
337 melanistic pattern visible by eye was very light and not discerned by the algorithm. To ensure a
338 robust pattern with enough spots to measure average characteristics, we included a spot
339 pattern only if the algorithm identified a minimum number of spots (at least 4 or 6 interior spots).
340 All of the geckos had patterning on the heads and tails, only two were missing patterns on the
341 trunk, and approximately half (13/25) of the geckos were missing patterns on their legs. There is
342 furthermore an identifiable hierarchy of patterning {head;tail}→ {trunk}→ {front legs;back legs} for
343 each individual gecko, where absence of patterns in one of the body parts entails absence of
344 patterning in all “downstream” body parts with respect to this hierarchy. For instance, absence
345 of patterning on the trunk means that all legs have no patterns as well. There was no clear
346 hierarchy between the front legs and back legs. Of those missing patterns on legs, most geckos
347 (7/13) were missing patterns on both sets of legs, 2 were missing patterns on their back legs
348 only, and 4 were missing patterns on their front legs only. Although our sample size is limited for
349 the “lemon frost” morph, there appeared to be an effect of morphotype: for the “normal”
350 morphotype, absence of patterns on the front legs always meant that the back legs were also
351 unpatterned, whereas this was reversed for this morph, since no gecko had patterned front legs.
352

353 Measurement error

354 We took four independent photos of each body part. To estimate the amount of measurement
355 error in each of the 14 indices, we took two different approaches (see Methods).

356 In the first, we consider body part patterns as points in 14-dimensional phenotype space
357 and measure the distances between them. We determined first the mean distance of the four
358 repeated measurements of the same body part of the same animal from their centroid. This is
359 an absolute measure of the measurement error. Table A1 in the Appendix lists these errors for
360 all seven body parts as well as the relative error as the ratio of these errors relative to i) the
361 mean *between-individual* distances for the same body part, or ii) the corresponding *within-*
362 *individual* distances for front or back legs (comparing the left and right leg of the same gecko).
363 The results for both the Mahalanobis distance and the Developmental Noise distance are listed.
364 In all cases, the mean within- or between-individual distances were significantly greater than the
365 mean distance due to the measurement error, with factors varying from 2.2 (back leg, within-
366 individual distance relative to measurement error, Mahalanobis distance) to 86.1 (tail, between-

367 individual distance relative to measurement error, Developmental Noise distance). A factor of 1
368 would mean that within- or between-individual distances were of the same magnitude (and thus
369 indistinguishable) from measurement error. However these distances were at least twice as
370 large (and often much larger), indicating that the measurement error is relatively small.

371 In the second approach for characterizing the measurement error, we conducted a two-
372 way ANOVA test where the two factors are “sides” (S; fixed) and “individuals” (I; random)
373 separately for both pairs of front legs and pairs of back legs for each of the 14 indices. This is a
374 standard approach to compare the relative contributions of nondirectional asymmetry
375 (biological) and measurement error (technical variation) in the investigation of paired structures
376 (Palmer and Strobeck, 1986; Merila and Biorklund, 1995; Breuker et al., 2006). For each index,
377 an F-test yielded that nondirectional asymmetry is making a significant contribution to the
378 variation observed relative to measurement error. The F-values had a median value of 6.8,
379 meaning that the measurement error made up about 15% (median value) of the total observed
380 variation between the left and right leg patterns. See Table A2 in the Appendix for details.
381

382 General pattern variation across geckos and body parts

383 For each body part of each of the 25 studied animals, we determined the value of each of the 14
384 indices listed in Table 3 via the mean of four repeated independent measurements.
385 An examination of the coefficient of variation (ratio of standard deviation and mean) for the 14
386 indices shows that melanistic pattern is highly variable for measures that concern the proportion
387 of melanistic areas (FM), how large these individual areas are (SA and SSD), and, to a lesser
388 extent, what their typical distances are from each other (PL and MD) (Table A4 in the Appendix).
389 This is not an artifact of the measurement error, which actually tended to be larger for MD than
390 the other indices by some measures (see Table A2). In essence, spots can be in higher or lower
391 density across geckos and body parts and larger or smaller. However, once a melanistic pattern
392 is established, the spots are all similar in shape (EE, EL). Table 4 displays the pairwise Pearson
393 correlation coefficients showing how much one index is correlated with another. For example,
394 measures of the size of spots such as FM, SS and SA are strongly positively correlated. The
395 two indices of the typical wavelength (roughly representing the typical distance among
396 melanistic areas), PL and MD, are also positively correlated. It is also noteworthy that EE, which
397 quantifies aspects of the shape of individual spots, is only weakly correlated with the other
398 indices, with the exception of the mean elongation (EL), which also quantifies aspects of the
399 shape of individual spots. This indicates that the spot shape only weakly depends on size or
400 distribution of the spots. A negative correlation value indicates that two indices are anti-
401 correlated. For example, fractional melanistic area (FM) and peak length (PL) are moderately
402 anti-correlated since fractional melanistic area – the proportion of melanistic area to total skin
403 area- tends to increase with the number of spots while peak length a measure of the typical
404 distance between spots - decreases with the number of spots. EE and EED are moderately anti-
405 correlated, which indicates that spots with large eccentricity tend to have a lower variation in
406 their eccentricity, which indicates an eccentricity that is non-random.

407 We also computed the correlation coefficients of within-individual indices of the various
408 body parts. The results are summarized in Table 5. A total of 127 out of the 294 correlation

409 coefficients were statistically significant at the 0.05 level of significance (39.8%), meaning that
410 we can statistically reject the hypothesis that variation of these indices is independent among
411 these body parts. The number of statistically significant coefficients varied substantially by the
412 pair of body parts. Correlation is significant for most indices for the two front leg patterns and the
413 head and tail patterns (FL-FR, HD-TA; each 11 out of 14). To a somewhat lesser extent, the
414 indices for the two back legs tended to be correlated (BL-BR; 9 out of 14 significant). Correlation
415 between front and back legs (FL-BL, FL-BR, FR-BL, FR-BR) was much weaker. The trunk
416 pattern was most strongly correlated with the tail pattern (TR-TA; 8 out of 14). Interestingly,
417 within-individual correlation tends to be weak for indices describing the typical shape of the spot
418 (EE, EL), whereas measures of the relative size of the spots (FM, SS, SA) tend to be highly
419 correlated between body parts.

420
421
422

423 We performed a principal component analysis on the 14 indices taken across all the 25
424 studied geckos and across the different body parts, the results of which are summarized in
425 Table A3 and Figures 4-6. A principal component analysis is a statistical method to convert a
426 set of observations (in our case, among 14 indices that have many overlaps in the information
427 they are describing) into a smaller number of uncorrelated variables called the principal
428 components. Together, the first seven components account for over 94% of the total variance
429 between the 132 different patterns we analyzed. The first principal component (explaining 45%
430 of the variance) has larger coefficients for those indices that are associated with the average
431 size of the spots, while the second component (18% of the variance) tends to have larger
432 coefficients for those indices associated with the characteristic wavelength (roughly
433 corresponding to the distance among spots) of the pattern. The third principal component (12%
434 of the variance) is strongly associated with EE and EED, which describes how close the
435 individual spots are to circular shapes, and how much they vary in this regard.

436 Figures 4-6 summarize the PCA data graphically. Together PC1 and PC2 (generally,
437 variation in spot size and separation, respectively) explain nearly two thirds of the pattern
438 variation (62.8%) and provide insight into systematic differences among patterns of the legs,
439 head, tail and trunk. Clusters of leg patterns are well separated and distinct from clusters of the
440 head and tail patterns for plots of PC1 versus PC2 (Figure 4). Since they sort along the PC1
441 axis (roughly, summarizing measures of spot size), we find that for example the head and tail
442 patterns tend to have larger average spot areas, while leg spots have smaller average spot
443 areas (Figure 5, top right and bottom left). This is true for both the absolute size of the spots
444 (indices SA and SS) as well as the size of the melanistic area as a fraction of total skin area
445 (FM), indicating that leg spots tend to be disproportionately smaller than body spots. When
446 looking at pattern variation only for legs, we observe that the front legs are clustered with lower
447 PC2 values (PC2 is more associated with measures corresponding to the distance among
448 spots) and also variation in the front legs tends to be smaller than variation in back legs (Figure
449 6, left).

450
451

452 Within-individual and between-individual distances in pattern
453 space - a measure of the influence of developmental noise in
454 pattern formation

455 **i. Pattern distances among pairs of legs**

456 We investigated whether the patterns on each pair of the four legs on each gecko are more
457 similar than the patterns on different geckos. In fact, variation in pattern among the two front
458 legs or the two back legs for each gecko most likely reflects the level of developmental noise in
459 pattern formation on the legs. In Figure 6 (left panel) – where variation reflects mostly
460 differences in the size of the spots and distance among them - a clustering of the legs of
461 individual geckos is not readily visible, suggesting that the contribution of noise generally is
462 more important than the contribution of genetic factors. It should be noted that although a
463 considerable measurement error also contributes to the differences between the legs, random
464 variation due to developmental noise is significantly larger than the measurement error (see
465 Tables A1 and A2). We compared the within-individual differences in pairs of leg patterns to the
466 between-individual differences in the same pairs (Figure 7). We found qualitatively somewhat
467 similar results for both the Mahalanobis distance (gray bars in Figure 7) and the Developmental
468 Noise distance (blue bars in Figure 7) concerning the distance between the two front legs and
469 the distance between the two back legs. In both cases, the within-individual distances were
470 smaller than the between-individual distances. Their ratio was between 0.55 and 0.57 for the
471 Mahalanobis distance and even 0.16-0.19 for the developmental noise metric (a ratio of 1.0
472 would indicate no difference between the within-individual and the between-individual
473 distances). The differences were highly statistically significant except for the case of back legs
474 and the Mahalanobis distance. The within-individual pair of the two front leg patterns is thus
475 found to be very significantly more similar than two leg patterns from different individuals.
476 (Statistical significance was assessed via nonparametric permutation tests, see the Appendix
477 for more details). Similarly, the within-individual distance between the two back leg patterns is
478 also found to be significantly smaller than the mean between-individual leg distance. For both
479 distances, a front leg and a back leg of the same gecko were closer to each other than a front
480 leg and a back leg patterns randomly taken from two different geckos. However, overall, the
481 mean distance between leg patterns of the same gecko is 64% of the mean distance between
482 patterns on different geckos for the Developmental Noise distance and 91% for the Mahalanobis
483 distance, a not statistically significant difference in the latter case. This further indicates that
484 there is large variation in leg pattern (Figures 4 and 6), and specifically that the variation
485 observed between legs within each individual is only slightly less than the one observed among
486 individuals, consistent with the small within-individual correlation coefficients observed for some
487 indices (Table 5). Our results indicate that within each gecko, two front legs and the two back
488 legs are much more similar to each other than a front and a back leg. This would suggest that
489 the difference between a front and a back leg is not just due to developmental noise. In fact, the
490 results support the hypothesis that the mechanisms - including timing of it - of pattern formation
491 and/or regulation of pattern establishment are distinct for the front and back legs.

492
493

494 **ii. Within-individual and between-individual pattern distances among heads, trunks, tails**
495 **and legs**

496

497 We also investigated the distances between the head, trunk, tail, and leg patterns. The results
498 are summarized in Figure 8. The distances are scaled with the same factor as in Figure 7, i.e.
499 the average distance between the patterns of two legs from different geckos is scaled to 1. We
500 compared the within-individual and between-individual distances for all possible pairs of head,
501 trunk, tail and leg patterns.

502 The comparisons of leg patterns with other body parts (legs-head, legs-trunk, legs-tail)
503 yielded that the mean within-individual distance was slightly smaller than the mean between-
504 individual distances for both the Mahalanobis distance and the Developmental Noise distance.
505 However, the differences were relatively small, between 5% and 12% for the Mahalanobis
506 distance and 6% and 18% for the Developmental Noise metric. For the Mahalanobis distance,
507 these differences did not reach statistical significance. In other words, if you take a leg pattern of
508 one individual, the difference between this leg pattern and, say, the head pattern of the same
509 individual is on average not statistically significantly smaller than the difference to the head
510 pattern of a second individual. This is different for the tail, head and trunk patterns. For all three
511 pairs - trunk and tail; head and tail; head and trunk - the within-individual distance is
512 significantly less than the between-individual distance. This means that on average, the patterns
513 of any two body parts of the same animal, ~~e.g. the head and the trunk,~~ is more similar than two
514 patterns from different animals, e.g. the head pattern of one animal and the trunk pattern of
515 another animal. This holds true for both Mahalanobis and Developmental Noise distances.

516

517

518 **Discussion and Conclusions**

519

520 The goal of this paper was to develop tools and methods to quantitatively study skin pattern
521 variation within and between individuals. We developed a pipeline to collect the data from
522 images of live geckos and then computed various geometric indices to describe characteristics
523 of the patterns. Similar approaches have been taken for giraffe coat patterns (Lee et al., 2018)
524 and salmonid fish skin patterns (Miyazawa et al. 2010); however in our work, not only we
525 captured different aspects of pattern elements and look at variation for each of the elements, but
526 we also used two concepts of distances to quantify the degree of similarity of patterns as whole.

527

528 Our method is not only relevant for the analysis of experimental data, but also for the evaluation
529 of mathematical models of skin pattern formation. There are in fact many such models (e.g.
530 Murray, 2002; Cruywagen et al., 1992; Painter, 2001; Cooper et al., 2018; Kondo et al., 2009),
531 encoding various hypothesized mechanisms of pattern formation. It is far from straightforward to
532 rigorously compare the synthetic patterns these models generate to the real skin patterns due to
533 the complexity and irregularity of the patterns. Most authors typically either compare only one or
534 two indices, such as the typical wavelength of the pattern, or just rely on the judgment of human
535 pattern recognition. While this method of comparing patterns “by eye” lacks rigorous

536 quantification, in some ways it is arguably far more developed and sophisticated than current
537 methods of pattern comparison based on lower-dimensional, quantifiable measures. Therefore,
538 our method represents a hybrid approach in which numerous, not necessarily independent
539 measures (the 14 indices used in this work, considered as pattern elements) are chosen at the
540 discretion of a human, based on the pattern variation and characteristics that are perceived as
541 important. The values of these measures are then obtained using automatic methods and
542 mathematical definitions are used to supply suitable weights for the measures to define the
543 distances between patterns. This approach therefore permits to fully depict variation in
544 melanistic patterns within and among individuals and to quantify differences.

545

546 **Hierarchy of patterned body parts based on developmental sequence of melanistic** 547 **patterning**

548 We found an identifiable hierarchy of melanistic patterning head/ tail→ trunk→legs in the
549 studied leopard geckos; for example presence of patterns on the front legs also entails patterns
550 on the trunk, tail and head, but not necessarily on the back legs (Table 1). There is no clear
551 hierarchy between the front legs and the back legs, although for the "normal" geckos in our
552 sample, unpatterned front legs implied unpatterned back legs. These results point to a
553 corresponding order of the establishment of patterns during development: it appears that pattern
554 formation occurs simultaneously in an anterior-posterior and a proximal-distal direction, forming
555 first on the head, then on the trunk, followed by the legs. Patterning of the front legs and the
556 back legs appears to be independent, due to the independent presence of pattern, the low
557 correlation of the pattern indices (Table 5) and the fact that within-individual comparisons of
558 front and back legs yielded very similar results as between-individual comparisons (Figure 7).
559 Pattern formation and establishment on the tail appears to be based on a related mechanism as
560 the head and trunk, as indicated by the similarity of tail and head patterns, as well as tail and
561 trunk patterns. The observed hierarchy of patterning partially follows pigmentation development
562 in this species. Melanistic pigmentation in the leopard gecko starts to appear around the
563 developmental stage 40 (hatching occurs at stage 42) as a banded pattern on the body and
564 spots on the front legs (but not on the back legs) (Wise et al., 2009). At the beginning of
565 developmental stage 41, the banded pattern is clearly distinct across the body while a spotted
566 pattern occurs on the upper part of the front leg. However, by the end of this stage,
567 pigmentation is occurring across the whole body (Wise et al. 2009). Although the body (head,
568 trunk, and tail) of hatchling and juvenile leopard geckos generally presents a banded pattern,
569 this species undergoes ontogenetic color changes, with adults generally having a spotted
570 pattern (Figure 1) (Landová et al., 2013). Ontogenetic change in color pattern however does not
571 occur for the legs after hatching (see above). Therefore, head, tail, and trunk follow a process of
572 pattern development and establishment that is different from the one occurring on the legs, with
573 the pattern on the front legs establishing before the one of the back legs (Wise et al. 2009),
574 potentially explaining why absence of pattern is more common in the back legs than the front
575 legs and in the front legs more than in the rest of the body.

576


577 General pattern variation across geckos and body parts

578 [Variation and correlation among pattern indices](#)

579 We found large variation and strong correlation among indices related to the amount of
580 melanistic area and the density and size of the spots among the different studied geckos and
581 among the different body parts (Tables 4 and 5). Although variation in spot size across body
582 parts and among individuals may partially be related to size differences, this is less the case for
583 the fraction of melanistic area on the total area. Independently on the observed variation, once
584 spots are formed, their average shape is similar across individuals (Table A4), suggesting a
585 strong constraint on this pattern element (EE), which is also weakly correlated to the other
586 indices (Table 4). While variation in spot size and density has also been observed in other
587 organisms (e.g. Asai et al., 1999; Morgan et al., 2014; Rudh et al., 2007; Balogová and Uhrin,
588 2015; Druml et al., 2017), less is known about variation in spot shape. Potential genetic or
589 developmental mechanisms may have evolved to ensure maintenance of spot shape and low
590 variability of this trait. On the other hand, other elements of the spotted pattern (e.g., density and
591 size) may be freer to vary in a coordinated way – as suggested by the observed high positive
592 correlation between some indices. Future research could further investigate if low variation in
593 spot shape also occurs in other spotted vertebrates and if it is similarly achieved across
594 organisms. In zebrafish, different alleles of the *leopard* gene result in changes in spot size,
595 density, and connectivity among spots, suggesting that this gene may regulate the synthesis of
596 an activator in a model of reaction-diffusion pattern formation (Asai et al., 1999). Later studies
597 identified the role of *leopard* in regulating interaction among melanophores (or among
598 xanthophores) and in controlling boundary shape for the spots (reviewed in Kondo et al., 2009;
599 Singh and Nüsslein-Volhard, 2015). Similarly, in horses, two genes with different alleles
600 determine the occurrence and amount of melanistic spots on a white colored coat (Druml et al.,
601 2017). The availability of the leopard gecko genome (Xiong et al., 2016), the relative easiness to
602 breed this species, and the existence of CRISPR-Cas9 technology already tested to create
603 mutations in lizards (Rasys et al., 2019) will allow to develop future research to uncover the
604 genetic basis of variation in pattern elements in this species, similarly to what has been done for
605 mammals and other non-mammalian model species.

606

607 [Variation and correlation in pattern among body parts](#)

608 Phenotypic correlation among traits, in this case the  correlation of patterns among different body
609 parts of the same individual, may provide information on how these patterns are related
610 developmentally. Phenotypic correlation was investigated in two ways. The first is the standard
611 method of Pearson correlation coefficients for each pair of body parts and for each
612 measurement, summarized in Table 5. The second measure is the ratio of the mean within-
613 individual distance and the mean between-individual distance in pattern space for each pair of
614 body parts, summarized in Figures 7 and 8. Patterns on the legs are statistically almost
615 independent of patterning on the head, trunk and tail. In contrast, the similarity of head, trunk
616 and tail patterns, as well as the similarity of the two front legs and the two back legs for the
617 same animal are statistically significant for both metrics. The similarity of pattern variation
618 observed on the head, trunk and tail suggests that patterning mechanisms are most likely not
619 independent among these body parts, and the same holds for the two front legs and the two

620 back legs (Figures 7 and 8; see also Table 5 for each index separately). However, as melanistic
621 patterns in the legs, and especially the back legs, are more variable and independent in their
622 variation from the rest of the body, this may indicate a different timing or developmental
623 mechanisms of pattern formation and establishment in these body parts. In this sense, the
624 relatively easiness of captive-breeding of this species may provide a unique opportunity into
625 understanding the underlying genetic and developmental processes and mechanisms producing
626 the the observed variation in color pattern in the different body parts (for similar questions, see
627 Cieslak et al., 2011; Druml et al., 2017; Wasik et al., 2014).

628

629 Comparison of within-individual and between-individual 630 differences in leg patterns as a measure of developmental noise.

631 A within-individual comparison of the two front leg patterns yields that the front legs of an
632 individual gecko are significantly more similar than two between-individual front leg patterns.
633 The same holds true for the two back legs. A simple measure of the magnitude of the
634 contribution of developmental noise is given by the ratio of the mean within-individual distance
635 and the mean between-individual distance, which is the amount of variation presumably due to
636 developmental noise alone normalized by the average amount of pattern variation due to all
637 sources (including genetic and environmental). A ratio of 0 would indicate that the legs of
638 individuals show no variation at all within a gecko, meaning that developmental noise plays no
639 part in the establishment of patterns at all. Conversely, a ratio of 1 would mean that the variation
640 between leg patterning of the same animal is indistinguishable to the variation between
641 patterning for two different animals. This would indicate that the process of patterning even
642 between geckos would be entirely dominated by random noise. In our data, the contribution of
643 developmental noise to patterning is quite large by this measure with ratios of within-individual
644 distances to between-individual distances between 0.55 and 0.16 or the Mahalanobis and
645 Developmental Noise metrics, respectively, for the front legs and 0.57 and 0.16 for the back
646 legs. While the measurement error contributes to this estimate - it accounts for between 47%
647 and 33% of the within-individual distances (Table A1) - the variation due to developmental noise
648 exceeds this error significantly (Tables A1 and A2). These indices indicate that although
649 variation in color pattern observed within individuals is not produced by developmental noise
650 alone, overall, developmental noise has a very strong influence on this variation. Together with
651 controlled captive-breeding experiments, the combination of mathematical modeling (see
652 section below) and empirical data can be used in the future to further investigate the relative
653 importance of genotype, environment and developmental noise on the variation in color pattern
654 on the different body parts in these animals. Furthermore, our methodological approach can
655 also be applied to other patterned organisms to study similar questions.
656

657 Methodological significance for the analysis of mathematical 658 models

659 Our method also serves the purpose of establishing a systematic high dimensional quantitative
660 approach to the analysis of synthetic patterns produced by mathematical models of skin pattern
661 formation (see e.g., Murray, 2002; Cruywagen et al., 1992; Painter, 2001; Cooper et al., 2018;
662 Kondo et al., 2009). Indeed, the distance between synthetic patterns and the actual patterns is
663 a quantifiable overall measure of how similar the synthetic patterns produced by such models
664 are to the actual patterns. More importantly, our method gives a way to quantify the effect of
665 developmental noise on patterns, which in turn can be used to calibrate and test mathematical
666 models of skin pattern formation. More concretely, we can think of the two front leg patterns of
667 an animal as two points in our 14-dimensional pattern space. The two leg patterns are similar,
668 but not identical. These two points represent the variation from a “typical” pattern that
669 corresponds to the environmental and genetic conditions of the particular individual’s
670 development. We postulate the differences between the two legs to be the effect of
671 developmental noise. Indeed, we can conceptualize abstract sets of possible patterns that can
672 be attained under the same combination of environmental and genetic conditions, but with the
673 random contribution of developmental noise. In a previous work, we have called this set a
674 ‘phenotype cloud’ (Kiskowski et al. 2019); see Figure 9 below. In our case, it is a subset of a 14-
675 dimensional pattern space. These phenotype clouds can be interpreted as confidence regions
676 for the phenotypes of individuals with the same genetics and similar environments, extending
677 the ideas of confidence intervals to higher dimensions. One can think for example of a 95%
678 phenotype cloud as an abstract set of patterns that contains a randomly generated pattern (with
679 fixed environmental and genetic conditions, but a random contribution of developmental noise)
680 in 95% of the cases. Since the distribution function for random noise is completely unknown,
681 and we only have two sample points for each instance - the pairs of front legs or the pairs of
682 back legs for each individual- , the actual shapes of these phenotype clouds are unclear.
683 However, in the context of stochastic mathematical models of pattern formation, such model-
684 dependent phenotype clouds can be determined computationally (Kiskowski et al. 2019), which
685 then allows us to test such model prediction against the empirical data.

686 Thus our approaches can be used to test the validity of mathematical models for skin
687 patterning, and gain insights and formulate prediction on the cellular and genetic mechanisms of
688 pattern formation (e.g., Maini, 2004; Othmer et al., 2009). Besides providing a framework for
689 quantitatively analyzing various aspects of patterns, the concept of the phenotype cloud gives
690 an additional empirical approach to interrogating models.

691

692

693

694 Acknowledgements

695 We are thankful to Gopal Murali, William Allen, and Julien Claude for discussing the correlation
696 of color pattern among distinct body parts in animals during the early phases of writing this
697 article. Julian Claude also provided helpful comments to improve this article. We also thank
698 Ekkehard Glimm for very helpful discussions about the statistical analysis, in particular for
699 discussions about computations of p-values. We are thankful to Tony Gamble, Aaron Griffing,
700 and John Scarbrough of Geckoboa for discussion about color pattern and color pattern selection
701 in the pet trade for the leopard gecko and to Matt Vickaryous for discussion about melanistic
702 color pattern formation, especially in regenerated tissues.

703

704

705 **References**

706 Allen, W.L., Moreno, N., Gamble, T., and Chiari, Y. (2020). Ecological, behavioral, and
707 phylogenetic influences on the evolution of dorsal color pattern in geckos. *Evolution* 74, 1033-
708 1047

709

710 Asai, R., Taguchi, E., Kume, Y., Saito, M., and Kondo, S. (1999). Zebrafish Leopard gene as a
711 component of the putative reaction-diffusion system. *Mechanisms of Development* 89, 87–92.

712

713 Bainbridge, H.E., Brien, M.N., Morochz, C., Salazar, P.A., Rastas, P., and Nadeau, N.J. Limited
714 genetic parallels underlie convergent evolution of quantitative pattern variation in mimetic
715 butterflies. *Journal of Evolutionary Biology* 33, 1516–1529.

716

717 Balogová, M., and Uhrin, M. (2015). Sex-biased dorsal spotted patterns in the fire salamander
718 (*Salamandra salamandra*). *Salamandra* 51, 12–18.

719

720 Belleghem, S.M.V., Papa, R., Ortiz-Zuazaga, H., Hendrickx, F., Jiggins, C.D., McMillan, W.O.,
721 and Counterman, B.A. (2018). patternize: An R package for quantifying colour pattern variation.
722 *Methods in Ecology and Evolution* 9, 390–398.

723

724 Berg, C.P. van den, Troscianko, J., Endler, J.A., Marshall, N.J., and Cheney, K.L. (2020).
725 Quantitative Colour Pattern Analysis (QCPA): A comprehensive framework for the analysis of
726 colour patterns in nature. *Methods in Ecology and Evolution* 11, 316–332.

727

728 Breuker, C.J., Patterson, J.S., and Klingenberg, C.P. (2006a). A Single Basis for Developmental
729 Buffering of *Drosophila* Wing Shape. *PLOS ONE* 1, e7.

730

731

732 Caro, T. (2005). The Adaptive Significance of Coloration in Mammals. *BioScience* 55, 125–136.

733

734 Chang, C., Wu, P., Baker, R.E., Maini, P.K., Alibardi, L., and Chuong, C.-M. (2009). Reptile
735 scale paradigm: Evo-Devo, pattern formation and regeneration. *Int J Dev Biol* 53, 813–826.

736

737 Cieslak, M., Reissmann, M., Hofreiter, M., and Ludwig, A. (2011). Colours of domestication.
738 *Biological Reviews* 86, 885–899.

- 739
740 Cooper, R.L., Thiery, A.P., Fletcher, A.G., Delbarre, D.J., Rasch, L.J., and Fraser, G.J. (2018).
741 An ancient Turing-like patterning mechanism regulates skin denticle development in sharks.
742 Science Advances 4, eaau5484.
743
744 Cruywagen, G.C., Maini, P.K., and Murray, J.D. (1992). Sequential pattern formation in a model
745 for skin morphogenesis. IMA J Math Appl Med Biol 9, 227–248.
746
747 Domingos, P. (2012). A few useful things to know about machine learning. Commun. ACM 55,
748 78–87.
749
750 Druml, T., Grilz-Seger, G., Neuditschko, M., Neuhauser, B., and Brem, G. (2017). Phenotypic
751 and Genetic Analysis of the Leopard Complex Spotting in Noriker Horses. J Hered 108, 505–
752 514.
753
754 Forsman, A., Ahnesjö, J., Caesar, S., and Karlsson, M. (2008). A Model of Ecological and
755 Evolutionary Consequences of Color Polymorphism. Ecology 89, 34–40.
756
757 Gomez, D., Théry, M., and Losos, E.J.B. (2007). Simultaneous Crypsis and Conspicuousness in
758 Color Patterns: Comparative Analysis of a Neotropical Rainforest Bird Community. The
759 American Naturalist 169, S42–S61.
760
761 Guo, L., Bloom, J.S., Sykes, S., Huang, E., Kashif, Z., Pham, E., Ho, K., Alcaraz, A., Xiao, X.G.,
762 Duarte-Vogel, S., et al. (2020). Genetics of white color and iridophoroma in “Lemon Frost”
763 leopard geckos. BioRxiv 2020.12.18.423549.
764 Kiskowski, M., Glimm, T., Moreno, N., Gamble, T., and Chiari, Y. (2019). Isolating and
765 quantifying the role of developmental noise in generating phenotypic variation. PLOS
766 Computational Biology 15, e1006943.
767
768 Kondo, S., Iwashita, M., and Yamaguchi, M. (2009). How animals get their skin patterns: fish
769 pigment pattern as a live Turing wave. Int. J. Dev. Biol. 53, 851–856.
770
771 Krzanowski, W.J. (2000). Principles of Multivariate Analysis (Oxford University Press).
772 Landová, E., Jančúchová-Lásková, J., Musilová, V., Kadochová, Š., and Frynta, D. (2013).
773 Ontogenetic switch between alternative antipredatory strategies in the leopard gecko
774 (*Eublepharis macularius*): defensive threat versus escape. Behav Ecol Sociobiol 67, 1113–
775 1122.
776
777 Lee, D.E., Cavener, D.R., and Bond, M.L. (2018). Seeing spots: quantifying mother-offspring
778 similarity and assessing fitness consequences of coat pattern traits in a wild population of
779 giraffes (*Giraffa camelopardalis*). PeerJ 6, e5690.
780
781 Mahalanobis, P.C. (1927). Analysis of race-mixture in Bengal. Journal of the Asiatic Society of
782 Bengal 23, 301–333.

783

784 Maini, P.K. (2004). Using mathematical models to help understand biological pattern formation.
785 *Comptes Rendus Biologies* 327, 225–234.

786

787 McGuirl, M.R., Volkening, A., and Sandstede, B. (2020). Topological data analysis of zebrafish
788 patterns. *PNAS* 117, 5113–5124.

789

790 Merila, J., and Biorklund, M. (1995). Fluctuating Asymmetry and Measurement Error.
791 *Systematic Biology* 44, 97–101.

792

793 Miura, T., Komori, M., and Shiota, K. (2000). A novel method for analysis of the periodicity of
794 chondrogenic patterns in limb bud cell culture: correlation of in vitro pattern formation with
795 theoretical models. *Anat Embryol* 201, 419–428.

796

797 Miyazawa, S., M. Okamoto, S. Kondo, (2010). Blending of animal colour patterns by
798 hybridization. *Nat. Commun.* 1, 66.

799

800 Morgan, S.K., Pugh, M.W., Gangloff, M.M., and Siefferman, L. (2014). The Spots of the Spotted
801 Salamander Are Sexually Dimorphic. *Cope* 2014, 251–256.

802

803 Murali, G., Merilaita, S., and Kodandaramaiah, U. (2018). Grab my tail: evolution of dazzle
804 stripes and colourful tails in lizards. *Journal of Evolutionary Biology* 31, 1675–1688.

805

806 Murray, J.D. (2002). *Mathematical biology. II* (New York: Springer-Verlag).

807

808 Murren, C.J. (2012). The Integrated Phenotype. *Integr Comp Biol* 52, 64–76.

809

810 Olsson, M., Stuart-Fox, D., and Ballen, C. (2013). Genetics and evolution of colour patterns in
811 reptiles. *Seminars in Cell & Developmental Biology* 24, 529–541.

812

813 Othmer, H.G., Painter, K., Umulis, D., and Xue, C. (2009). The Intersection of Theory and
814 Application in Elucidating Pattern Formation in Developmental Biology. *Mathematical Modelling*
815 *of Natural Phenomena* 4, 3–82.

816

817 Painter, K.J. (2001). Models for Pigment Pattern Formation in the Skin of Fishes. In
818 *Mathematical Models for Biological Pattern Formation*, P.K. Maini, and H.G. Othmer, eds. (New
819 York, NY: Springer), pp. 59–81.

820

821 Palmer, A.R., and Strobeck, C. (1986). Fluctuating Asymmetry: Measurement, Analysis,
822 *Patterns*. *Annual Review of Ecology and Systematics* 17, 391–421.

823

824 Pérez I de Lanuza, G.P. i de, and Font, E. (2016). The evolution of colour pattern complexity:
825 selection for conspicuousness favours contrasting within-body colour combinations in lizards.
826 *Journal of Evolutionary Biology* 29, 942–951.

827

828 Prinsloo, N.D., Postma, M., and de Bruyn, P.J.N. How unique is unique? Quantifying geometric
829 differences in stripe patterns of Cape mountain zebra, *Equus zebra zebra* (Perissodactyla:
830 Equidae). *Zoological Journal of the Linnean Society* 191, 612–625.

831

832 Rasys, A.M., Park, S., Ball, R.E., Alcala, A.J., Lauderdale, J.D., and Menke, D.B. (2019).
833 CRISPR-Cas9 Gene Editing in Lizards through Microinjection of Unfertilized Oocytes. *Cell*
834 *Reports* 28, 2288-2292.e3.

835

836 Rudh, A., Rogell, B., and Höglund, J. (2007). Non-gradual variation in colour morphs of the
837 strawberry poison frog *Dendrobates pumilio*: genetic and geographical isolation suggest a role
838 for selection in maintaining polymorphism. *Molecular Ecology* 16, 4284–4294.

839

840 Singh, A.P., and Nüsslein-Volhard, C. (2015). Zebrafish Stripes as a Model for Vertebrate
841 Colour Pattern Formation. *Current Biology* 25, R81–R92.

842

843 Solan, T. de, Renoult, J.P., Geniez, P., David, P., and Crochet, P.-A. (2019). Looking for
844 mimicry in a snake assemblage using deep learning. *BioRxiv* 789206.

845

846 Szydłowski, P., Madej, J.P., Duda, M., Madej, J.A., Sikorska-Kopyłowicz, A., Chełmońska-Soyta,
847 A., Ilnicka, L., and Duda, P. (2020). Iridophoroma associated with the Lemon Frost colour morph
848 of the leopard gecko (*Eublepharis macularius*). *Scientific Reports* 10, 5734.

849

850 Tibbetts, E.A., and Dale, J. (2004). A socially enforced signal of quality in a paper wasp. *Nature*
851 432, 218–222.

852

853 Troscianko, J., Skelhorn, J., and Stevens, M. (2017). Quantifying camouflage: how to predict
854 detectability from appearance. *BMC Evol Biol* 17, 7.

855

856 Wasik, B.R., Liew, S.F., Lilien, D.A., Dinwiddie, A.J., Noh, H., Cao, H., and Monteiro, A. (2014).
857 Artificial selection for structural color on butterfly wings and comparison with natural evolution.
858 *PNAS* 111, 12109–12114.

859

860 Wise, P.A.D., Vickaryous, M.K., and Russell, A.P. (2009). An Embryonic Staging Table for In
861 Ovo Development of *Eublepharis macularius*, the Leopard Gecko. *The Anatomical Record* 292,
862 1198–1212.

863

864 Xiong, Z., Li, F., Li, Q., Zhou, L., Gamble, T., Zheng, J., Kui, L., Li, C., Li, S., Yang, H., et al.
865 (2016). Draft genome of the leopard gecko, *Eublepharis macularius*. *GigaScience* 5, 47.

866

867 Zerdoumi, S., Sabri, A.Q.M., Kamsin, A., Hashem, I.A.T., Gani, A., Hakak, S., Al-garadi, M.A.,
868 and Chang, V. (2018). Image pattern recognition in big data: taxonomy and open challenges:
869 survey. *Multimed Tools Appl* 77, 10091–10121.

870

Figure 1

Figure 1: Example gecko image

Adult leopard gecko (animal #21003). Note the differences in patterning on the head, trunk, legs and tail.

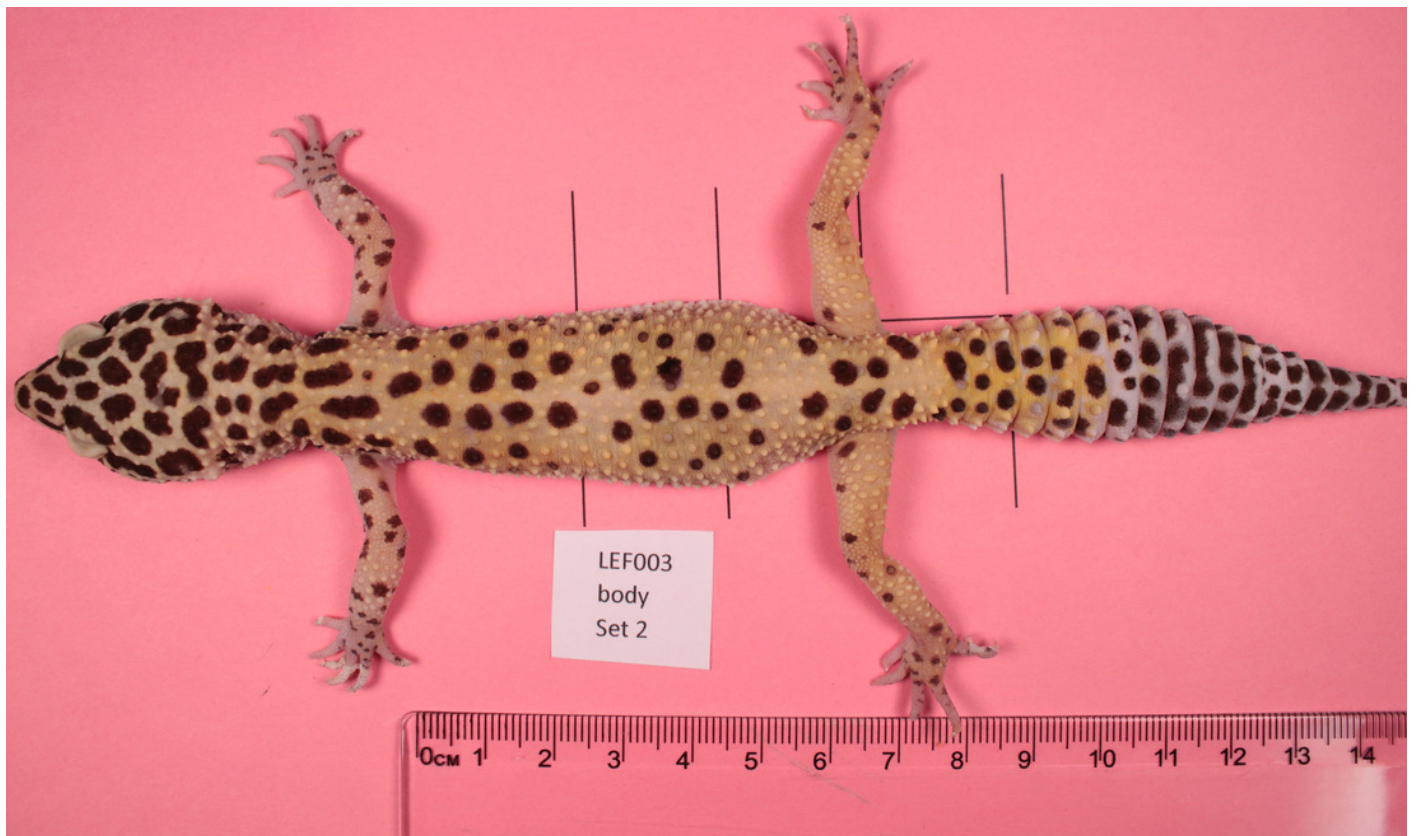


Figure 2

Figure 2: Body parts

Outline of the gecko body showing the seven regions of patterns that were isolated from gecko images. Each region was photographed separately, and the limbs were gently stretched during photographing. Nevertheless, depending on the gecko configuration, viewing angles and the region shapes were irregular. An image processing algorithm was used to identify the pattern that was viewable within each region irrespective of the shape. The abbreviations BL (left back leg), BR (right back leg), FL (left front leg), FR (right front leg), HD (head), TR (trunk) and TA (tail) are as in Table 1 and are used throughout this article.

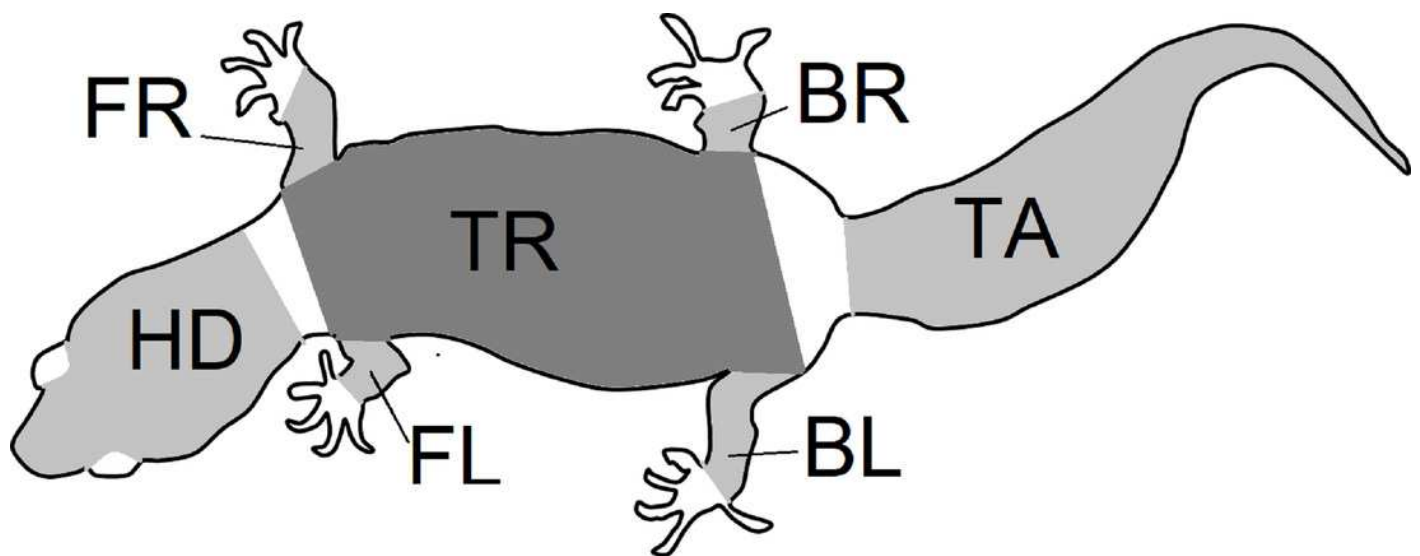


Figure 3

Figure 3: Flow chart

Flow chart of image acquisition and processing

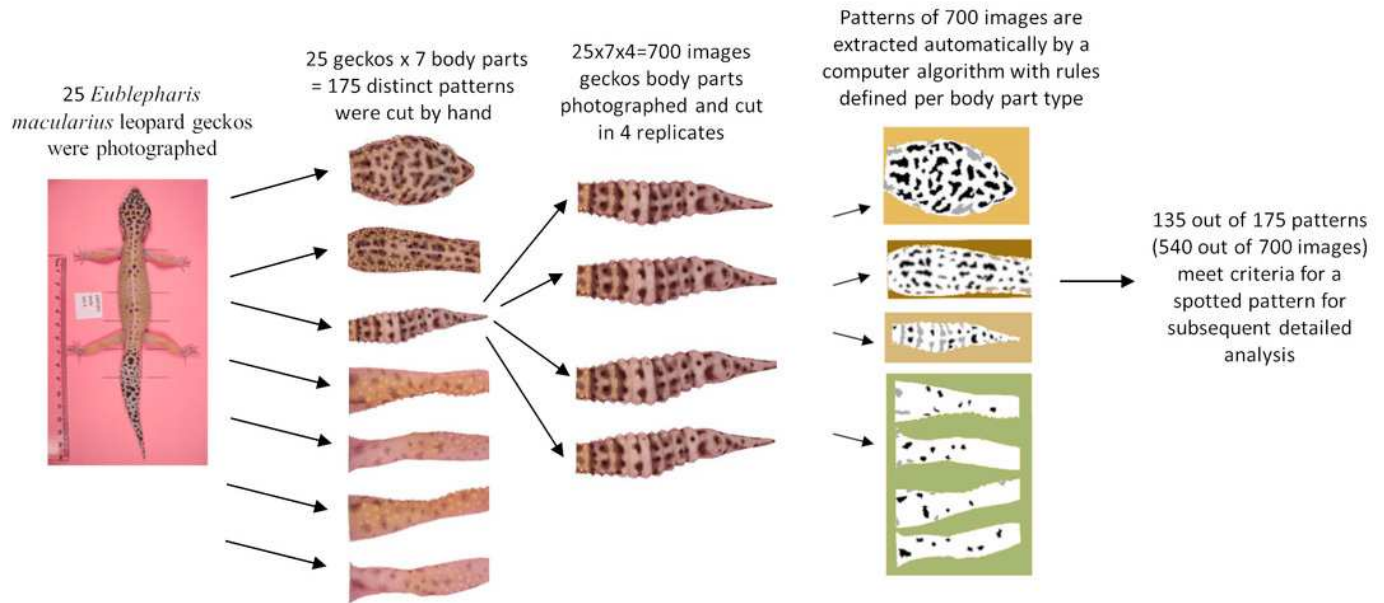


Figure 4

Figure 4: Data visualization 1

Plot of principal components 1 and 2. Each dot in the plot corresponds to a specific body part of a gecko. Body parts are colored coded and indicated by the same symbol as in Figure 2. A few outliers are labeled via the corresponding gecko id (See Figure A1 in the Appendix for images of all individuals. Note that the two outliers for the trunk patterns in the top left corner correspond to two normal morphs obtained from different sources, suggesting that grouping between these two individuals is not due to them being blood related). Data from all the 25 geckos with pattern in the specific body part indicated.

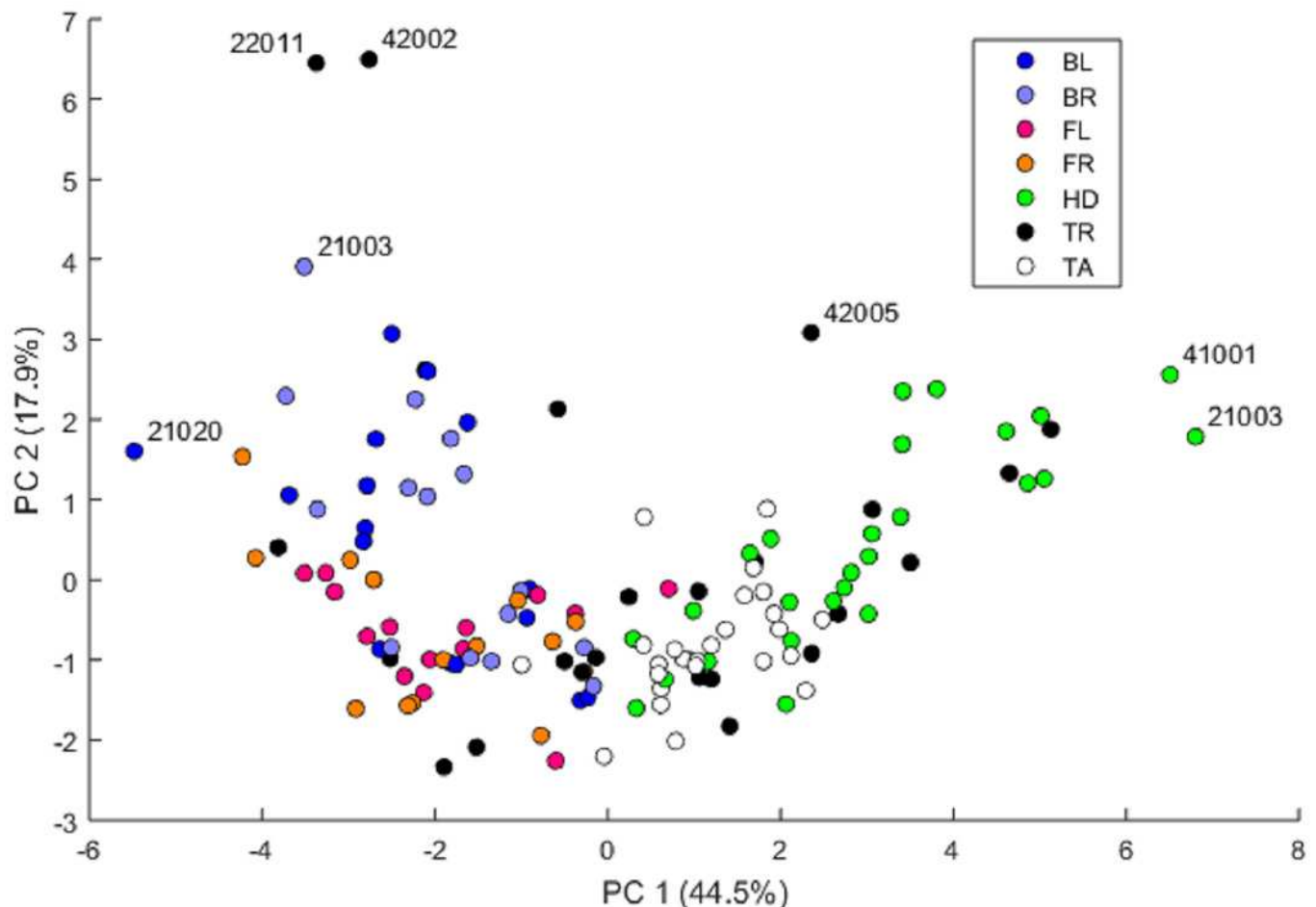


Figure 5

Figure 5: Data visualization 2

Plots of principal components 1 and 3 (top left); spot area (SA) vs. mean distance between neighboring spots (MD; top right); fractional area (FM) vs. spot diameter (SS; bottom left) and ellipticity (EE) vs. peak length (PL; bottom right). Percentages in parentheses give the fraction of the total standard deviation explained by the given principal component. Body parts are color coded as indicated in Figure 4. Axes bounds are chosen so that in some cases, a few outliers are not shown. Data from all the 25 geckos with pattern in the specific body part indicated.

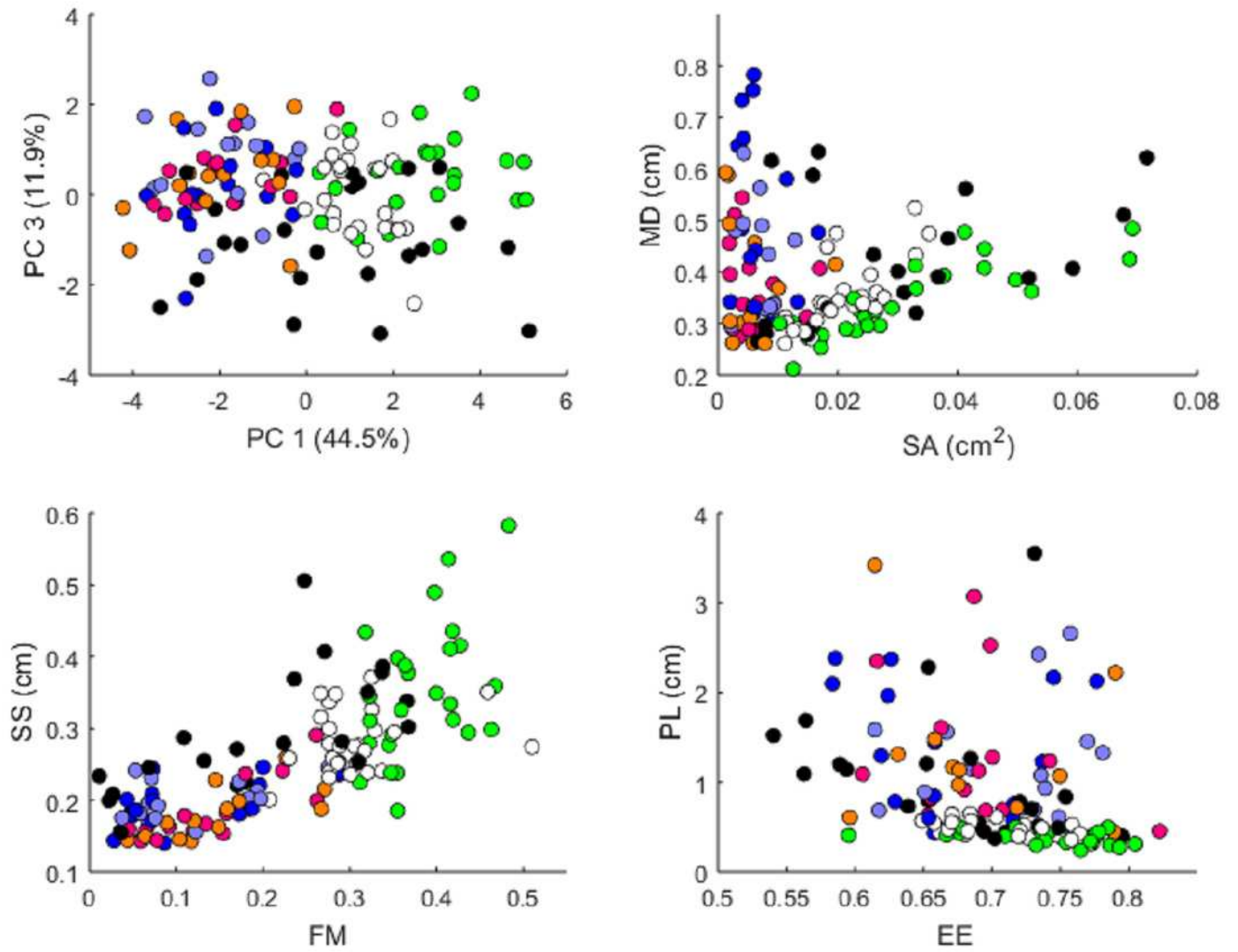


Figure 6

Figure 6: Data visualization 3

Left: Plot of principal components 1 and 2 of all leg patterns. Geckos are color coded as indicated in the legend and each dot in the plot corresponds to a specific leg of a gecko. The two back legs of the same gecko are connected via a blue line; the two front legs by a purple ('fuchsia') line. **Right:** Plot of principal components 1 and 2 of head (HD), trunk (TR) and tail (TA) patterns. Geckos are color coded by morph.

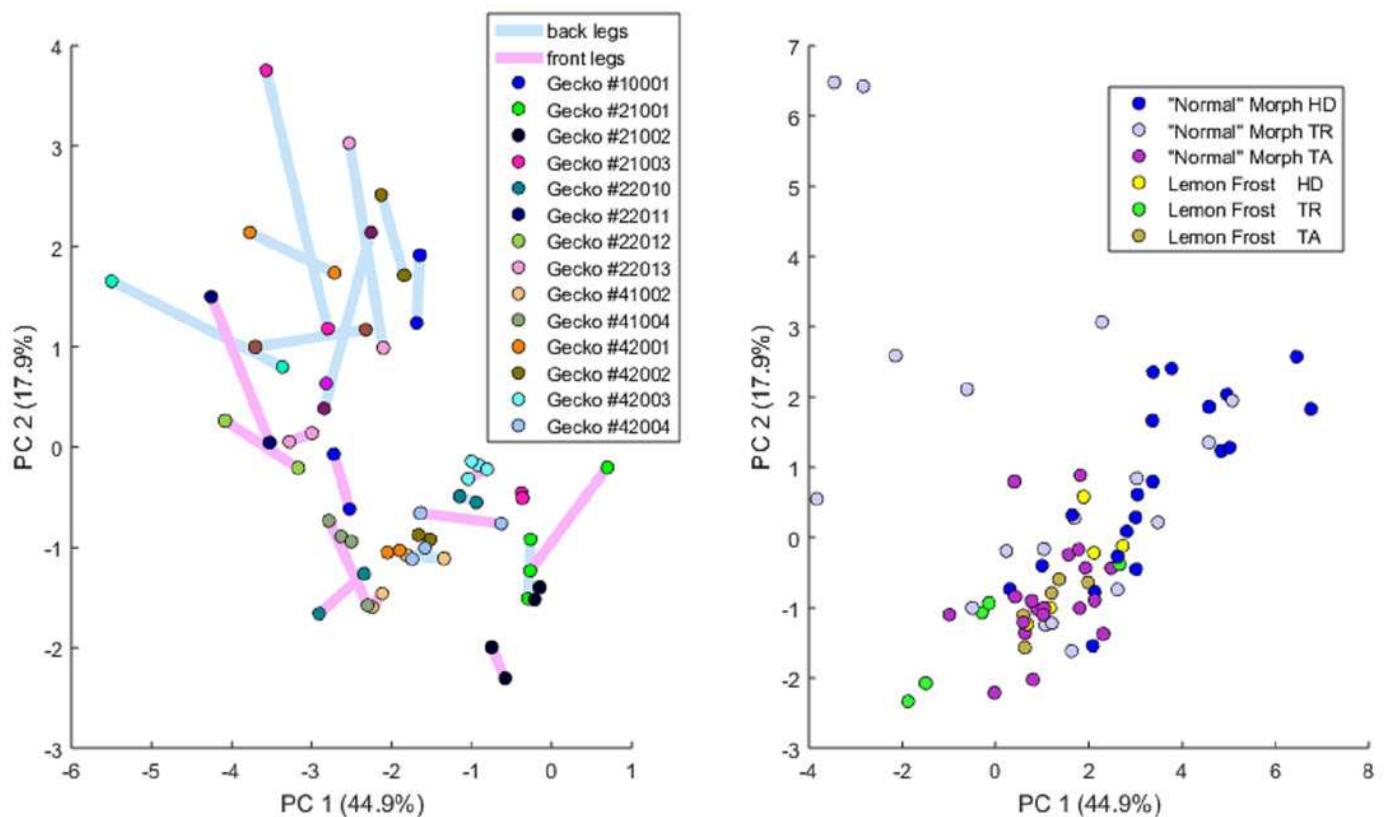


Figure 7

Figure 7: Distances of leg patterns

(Squared) distances among leg patterns. For each type of leg comparison, within individual distance (bars without stripes) and between individual distance (bars with stripes) and their ratio (value indicated above each pair of bars) are shown. Gray bars show the Mahalanobis distance, blue bars show the Developmental Noise distance (see inset below the figure). Distance squares are scaled so that the mean between-individual leg distance, i.e. the distance between two leg patterns of different individuals, is 1 in each metric. Stars are based on the p-values for the null hypothesis that the mean within-individual distance is greater or equal to the between-individual distance; equivalently, that the ratio between the two is greater or equal to one. The alternative hypothesis is that the mean within-individual distance is strictly less than the between-individual distance. Data obtained on all the 25 geckos together independently of morphotype. One star (*) indicates p-values less than 0.05, ** p-values less than 0.01, *** p-values less than 0.001, **** p-values less than 0.00001.

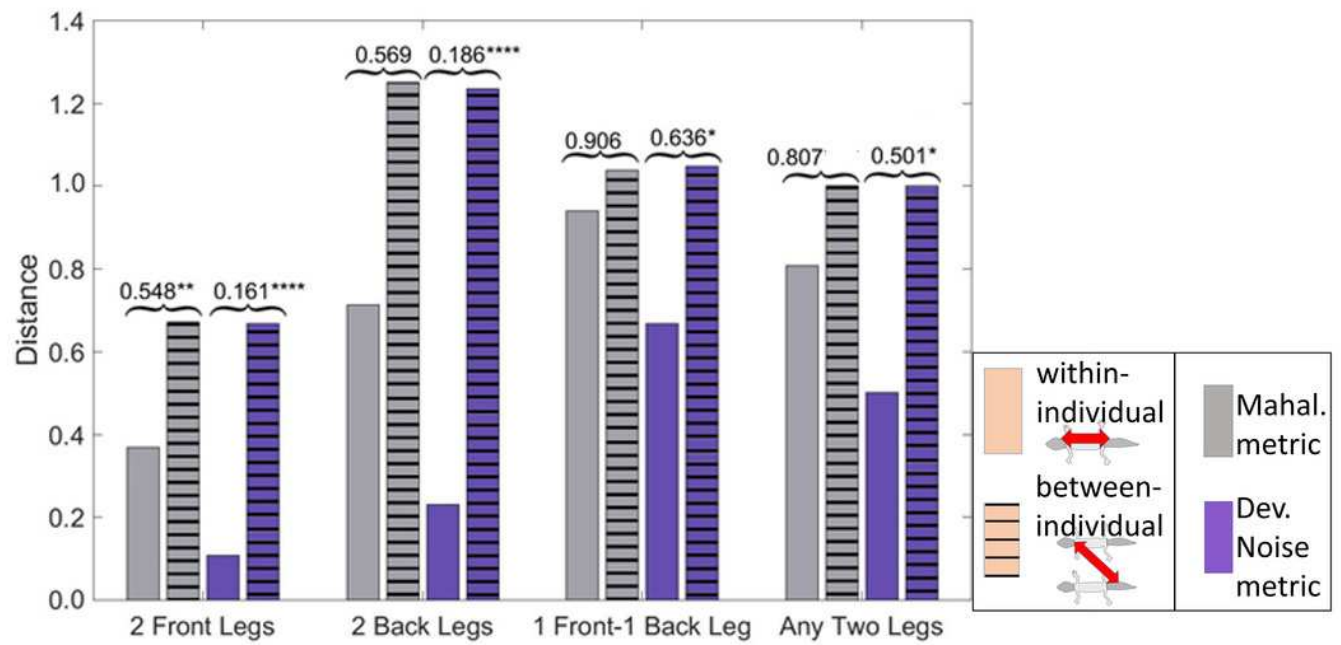


Figure 8

Figure 8: Distances of patterned body parts

(Squared) distances among head, trunk, tail, and (front) legs. For each type of leg comparison, within individual distance (bars without stripes) and between individual distance (bars with stripes) and their ratio (value indicated above each pair of bars) are shown. Blue bars show the Mahalanobis distance, gray bars show the Developmental Noise distance (see also the legend to Figure 7). Scaling of distances as in Figure 7. Stars are based on the p-values for the null hypothesis that the mean within-individual distance is greater or equal to the between-individual distance; equivalently, that the ratio between the two is greater or equal to one. The alternative hypothesis is that the mean within-individual distance is strictly less than the between-individual distance. One star (*) indicates p-values less than 0.05, ** p-values less than 0.01, *** p-values less than 0.001, **** p-values less than 0.00001. Data obtained on all the 25 geckos together independently of morphotype.

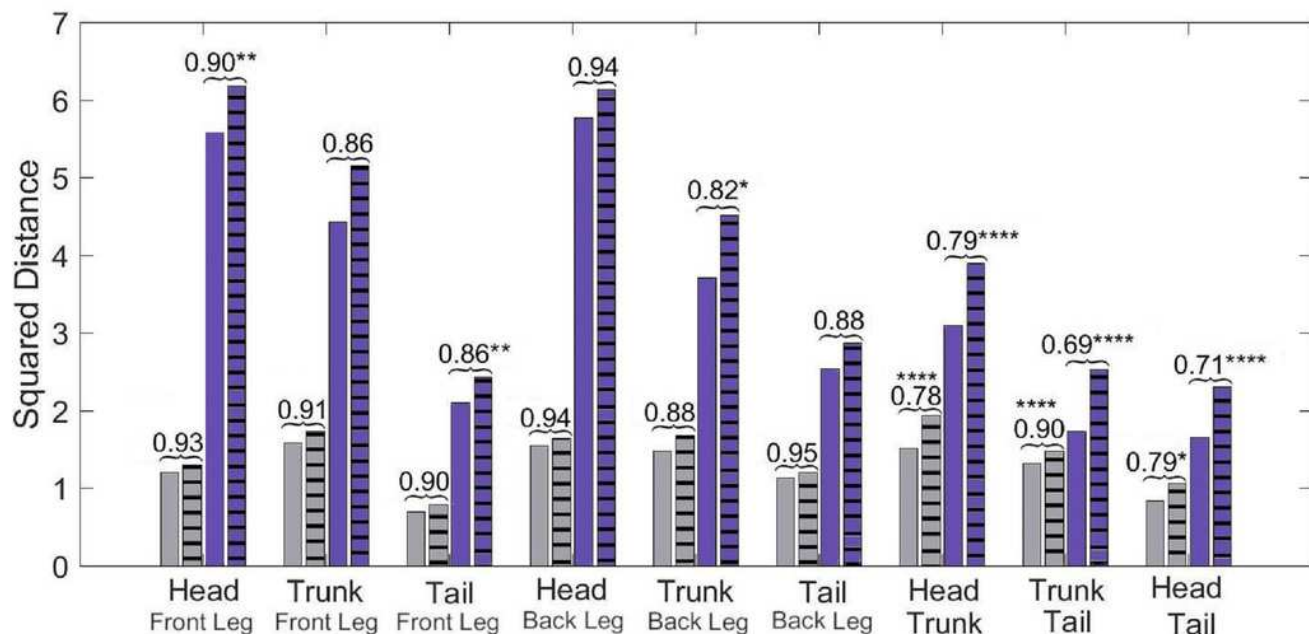


Figure 9

Figure 9: Visualization of phenotype cloud

Illustration of the concept of a “phenotype cloud”. The images show the gecko pattern data in FM-SS space (left) and PL-SA space (right). Each gecko corresponds to a unique color and the body part is indicated by a two letter-combination (see Figure 2). The ellipses shown are visualizations of the concept of phenotype clouds of gecko #10001 (indicated in bright red). In fact, these ellipses are projections of certain balls (with respect to the Developmental Noise metric) in 14-dimensional pattern space onto the FM-SS subspace (left) and on the SA-PL subspace (right). These balls are centered at the centroid of the two front leg patterns of gecko #10001 (indicated in bright red). The radius of the innermost ball is equal to the distance of one of the front legs to the centroid in the 14-dimensional pattern space. The other concentric balls have twice and three times this radius. Phenotype clouds can be conceptualized as such balls, e.g. the 95% phenotype cloud is a set that contains randomly generated patterns with the same environmental and genetic conditions and the same level of developmental noise as the front legs of gecko #10001 in 95% of the cases. While it is not possible to generate such phenotype clouds for a single pattern from our data empirically - we only have two data points for each cloud, corresponding to the left and right leg -, it is possible for stochastic mathematical models of pattern formation. The size of the cloud then indicates the contribution of developmental noise to pattern formation - the larger the cloud, the larger the influence of developmental noise.

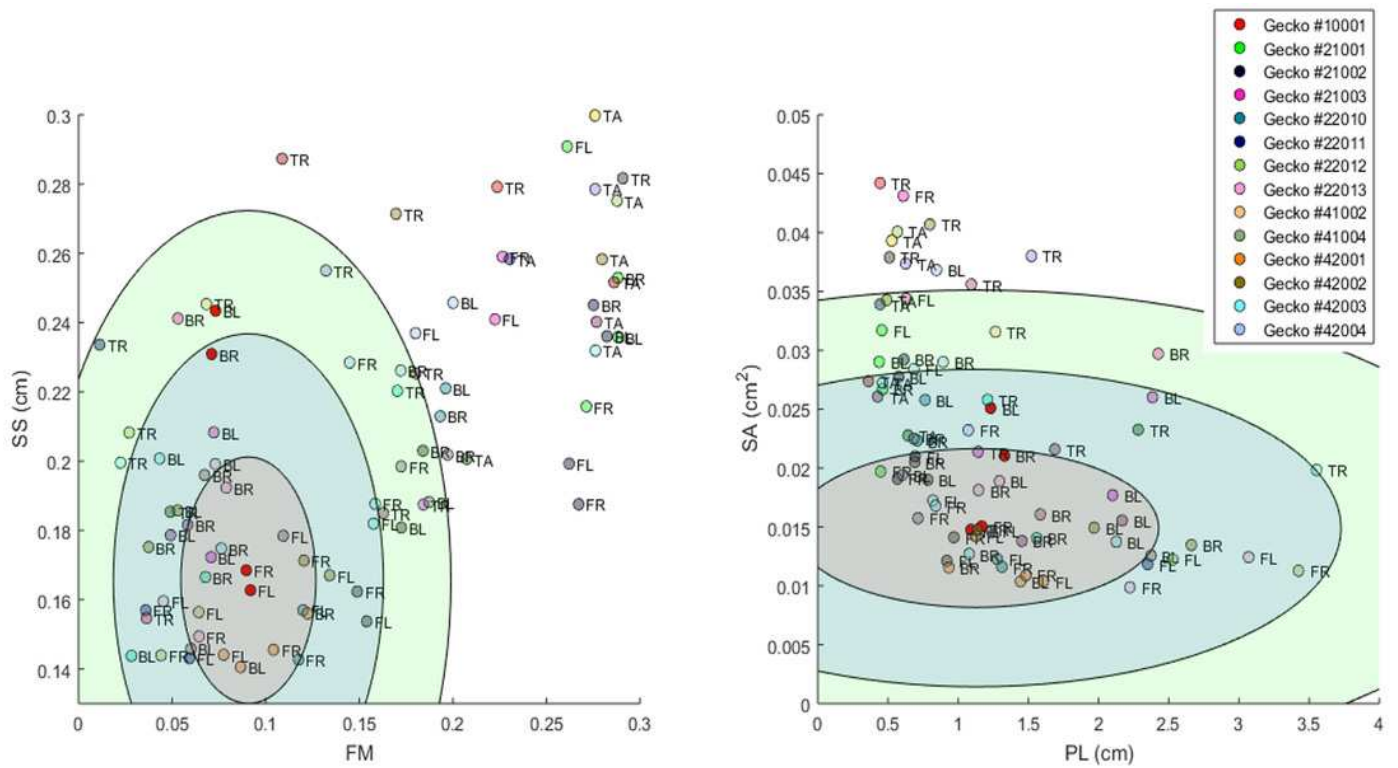


Table 1 (on next page)

Word file with all tables.

Please see the file "CAPTIONS_FOR_ALL_FIGURES_AND_TABLES" for the captions. (Attached in this PDF file after the tables.)

1 TABLES

2

	Morph	Source	ID	Sex	BL	BR	FL	FR	TR	HD	TA
1	Normal	w	10001	F	YES	YES	YES	YES	YES	YES	YES
2	Normal	g	21001	F	YES	YES	YES	YES	YES	YES	YES
3	Normal	g	21002	F	YES	YES	YES	YES	YES	YES	YES
4	Normal	g	21003	F	YES	YES	YES	YES	YES	YES	YES
5	Normal	g	22010	M	YES	YES	YES	YES	YES	YES	YES
6	Normal	b	22013	M	YES	YES	YES	YES	YES	YES	YES
7	Normal	b	41002	F	YES	YES	YES	YES	YES	YES	YES
8	Normal	b	41004	F	YES	YES	YES	YES	YES	YES	YES
9	Normal	b	42001	M	YES	YES	YES	YES	YES	YES	YES
10	Normal	b	42002	M	YES	YES	YES	YES	YES	YES	YES
11	Normal	b	42003	M	YES	YES	YES	YES	YES	YES	YES
12	Normal	b	42004	M	YES	YES	YES	YES	YES	YES	YES
13	Normal	g	22011	M	NO	NO	YES	YES	YES	YES	YES
14	Normal	b	22012	M	NO	NO	YES	YES	YES	YES	YES
15	Normal	w	10002	F	NO	NO	NO	NO	YES	YES	YES
16	Normal	g	21008	F	NO	NO	NO	NO	YES	YES	YES
17	Normal	b	41001	F	NO	NO	NO	NO	YES	YES	YES
18	Normal	b	42005	M	NO	NO	NO	NO	YES	YES	YES
19	Normal	g	21007	F	NO	NO	NO	NO	NO	YES	YES
20	Normal	b	41003	F	NO	NO	NO	NO	NO	YES	YES
21	LF	t	21019	F	YES	YES	NO	NO	YES	YES	YES
22	LF	t	21020	F	YES	YES	NO	NO	YES	YES	YES
23	LF	t	22016	M	YES	YES	NO	NO	YES	YES	YES
24	LF	t	22014	M	YES	NO	NO	NO	YES	YES	YES
25	LF	t	21018	F	NO	NO	NO	NO	YES	YES	YES

3

4 TABLE 1

5

6

7

8

Body Part	Channel Used to Compute	Channel and threshold Used to	Threshold
-----------	-------------------------	-------------------------------	-----------

Type	the Mean Pixel Intensity μ	Identify Shadows	
Limbs	Green	shadows: green $< \mu_G - 0.3\sigma_G$ glare: green $> \mu_G + 0.3\sigma_G$	maximum of these two quantities: $\mu_G - 0.85\sigma_G, 60$
Head	Green	N/A	maximum of these two quantities: $\mu_G - 0.50\sigma_G, 60$
Trunk	Green	shadows: blue $< \mu_B - 0.85\sigma_B$	maximum of these two quantities: $\mu_G - 0.85\sigma_G, 60$ additionally, maximally: 108
Tail	Green	N/A	maximum of these two quantities: $\mu_G - 0.85\sigma_G, 60$

9 **TABLE 2**

10

11

Abbr.	Name	Units	Description	Spot type used for the computation
FM	fraction of melanistic area	dimensionless	Ratio of black pixels to all pixels in binarized image (ratio of melanistic area to total area)	All Spots
SS	mean spot diameter ('spot size')	cm	Mean of the length of the major axes of the ellipses that have the same second moment as the spots (Matlab function <i>MajorAxisLength</i>)	Interior Spots
SSD	st.dev. of SS	cm	Standard deviation of the lengths of major axes used in definition of SS	Interior Spots
EE	mean ellipticity	dimensionless	Mean ratio of major axes to minor axes of ellipses that have the same second moment as the spots (Matlab function <i>Eccentricity</i>)	Interior Spots

EED	st. dev. of EE	dimensionless	Standard deviation of the ratios used in definition of EE	Interior Spots
PL	peak length	cm	Measure of characteristic wavelength; (typical distance between spots; see Miura et al. (2000))	All Spots
MD	mean minimum distance	cm	Mean of the mean distance of the centroid of a spot to the closest three other spots' centroids	All Spots
MDD	minimum distance st. dev.	cm	Standard deviation of the distances used in the definition of MD	All Spots
SA	spot area	cm ²	Mean area of spots	Interior Spots
SAD	st. dev. of spot area	cm ²	Standard deviation of the spot areas	Interior Spots
SI	spot intensity	dimensionless	Mean green values (G) of the RGB values of spots (between 0 and 255 for each pixel)	All Spots
SID	st. dev. of spot intensity	dimensionless	Standard deviation of the intensities used in the definition of SI	All Spots
EL	mean spot elongation	dimensionless	Mean of the spot elongation $EL = \frac{area}{2d^2}$ where d is the thickness of the spot (number of erosion steps needed before the pot disappears)	Interior Spots
ELD	st. dev. of spot elongation	dimensionless	Standard deviation of the spot elongation	Interior Spots

12 **TABLE 3**

13

14

15

16

	FM	SS	SSD	EE	EED	PL	MD	MDD	SA	SAD	SI	SID	EL	ELD
FM	1	0.76****	0.7****	0.39****	0.14	-0.63****	-0.5****	-0.65****	0.68****	0.62****	-0.76****	-0.55****	0.42****	0.45****
SS	0.76****	1	0.9****	0.42****	0.16	-0.39****	-0.063	-0.27**	0.97****	0.91****	-0.65****	-0.35****	0.57****	0.54****
SSD	0.7****	0.9****	1	0.38****	0.27**	-0.4****	-0.15	-0.28**	0.84****	0.93****	-0.55****	-0.36****	0.6****	0.64****
EE	0.39****	0.42****	0.38****	1	-0.47****	-0.4****	-0.061	-0.14	0.26**	0.29***	-0.094	-0.26**	0.58****	0.37****
EED	0.14	0.16	0.27**	-0.47****	1	-0.004	-0.1	-0.097	0.18*	0.19*	-0.2*	-0.079	-0.0041	0.15
PL	-0.63****	-0.39****	-0.4****	-0.4****	-0.004	1	0.63****	0.58****	-0.33***	-0.34****	0.35****	0.35****	-0.29***	-0.3***
MD	-0.5****	-0.063	-0.15	-0.061	-0.1	0.63****	1	0.85****	-0.029	-0.06	0.28***	0.36****	0.12	-0.011
MDD	-0.65****	-0.27**	-0.28**	-0.14	-0.097	0.58****	0.85****	1	-0.23**	-0.21*	0.49****	0.47****	0.082	0.022
SA	0.68****	0.97****	0.84****	0.26**	0.18*	-0.33***	-0.029	-0.23**	1	0.93****	-0.64****	-0.29***	0.45****	0.44****
SAD	0.62****	0.91****	0.93****	0.29***	0.19*	-0.34****	-0.06	-0.21*	0.93****	1	-0.58****	-0.3***	0.52****	0.54****
SI	-0.76****	-0.65****	-0.55****	-0.094	-0.2*	0.35****	0.28***	0.49****	-0.64****	-0.58****	1	0.46****	-0.11	-0.18*
SID	-0.55****	-0.35****	-0.36****	-0.26**	-0.079	0.35****	0.36****	0.47****	-0.29***	-0.3***	0.46****	1	-0.11	-0.068
EL	0.42****	0.57****	0.6****	0.58****	-0.0041	-0.29***	0.12	0.082	0.45****	0.52****	-0.11	-0.11	1	0.9****
ELD	0.45****	0.54****	0.64****	0.37****	0.15	-0.3***	-0.011	0.022	0.44****	0.54****	-0.18*	-0.068	0.9****	1

	FM	SS	SSD	EE	EED	PL	MD	MDD	SA	SAD	SI	SID	EL	ELD
FL-FR	0.95****	0.84***	0.48	0.4	-0.26	0.78**	0.89****	0.78**	0.85****	0.86****	0.98****	0.56*	0.7**	0.74**
HD-TA	0.7****	0.43*	0.51**	0.19	0.011	0.64***	0.72****	0.45*	0.53**	0.58**	0.65***	0.5*	0.53**	0.4
BL-BR	0.98****	0.81***	-0.09	0.45	-0.36	0.43	0.85****	0.77***	0.91****	0.73**	0.96****	0.79***	0.64*	0.33
FR-HD	0.89****	0.57*	0.45	0.017	-0.0058	0.42	0.66**	0.56*	0.79***	0.72**	0.84***	0.56*	0.12	0.28
TR-TA	0.71***	0.61**	0.45*	0.15	0.27	0.17	0.34	0.34	0.67***	0.43*	0.56**	0.6**	0.53**	0.2
BL-TR	0.85****	0.61*	0.05	0.29	0.34	0.29	0.61*	0.22	0.6*	0.42	0.84****	0.037	0.57*	0.16
HD-TR	0.66**	0.41	0.16	0.67***	0.38	0.26	0.61**	0.39	0.37	0.052	0.66**	0.32	0.57**	0.45*
BL-HD	0.52*	0.43	0.23	0.18	-0.15	0.12	0.83****	0.57*	0.33	0.17	0.67**	0.51*	0.29	-0.12
BR-TR	0.81***	0.54*	0.17	0.043	-0.14	0.2	0.4	0.24	0.64**	0.62*	0.73**	-0.063	0.3	0.2
FL-HD	0.81***	0.31	0.28	-0.14	-0.22	0.36	0.62*	0.29	0.56*	0.57*	0.9****	0.17	0.19	0.37
FL-TA	0.65*	0.48	0.62*	0.44	-0.18	0.4	0.64*	0.56*	0.45	0.46	0.67**	-0.096	0.19	0.34
FR-TR	0.61*	0.25	0.4	0.54*	-0.00097	0.8***	0.63*	0.28	0.37	0.33	0.66*	0.13	0.16	0.2
BL-FL	0.61*	0.56	-0.21	-0.2	-0.43	0.064	0.56	0.67*	0.68*	0.2	0.84***	-0.068	-0.22	-0.52
BL-FR	0.65*	0.41	0.008	0.13	0.15	0.13	0.64*	0.67*	0.44	0.15	0.84***	0.083	0.014	-0.46
BL-TA	0.71**	0.54*	-0.023	0.3	0.21	0.31	0.47	0.71**	0.52*	0.35	0.45	0.34	0.16	-0.4
BR-FR	0.62*	0.59*	0.11	-0.3	-0.36	0.066	0.44	0.18	0.62*	0.25	0.84***	0.15	-0.05	-0.23
BR-HD	0.53*	0.32	-0.4	0.18	0.024	0.5	0.74**	0.57*	0.38	-0.0023	0.61*	0.3	0.24	0.18
FR-TA	0.69**	0.39	0.14	0.22	0.21	0.19	0.64*	0.8***	0.44	0.38	0.7**	0.13	0.16	0.12
BR-FL	0.54	0.71**	0.38	-0.24	0.48	0.01	0.32	0.32	0.74**	0.33	0.82**	0.033	-0.022	-0.081
BR-TA	0.7**	0.74**	0.33	0.11	0.21	0.47	0.36	0.48	0.61*	0.38	0.46	0.048	0.3	0.23
FL-TR	0.5	0.27	0.28	-0.16	-0.53	0.54*	0.55*	0.33	0.41	0.31	0.65*	0.058	0.11	0.47

19

20 **TABLE 5**

21

	back legs		front legs		head		trunk		tail	
absolute measurement error (mean distance to centroid)	0.39	0.11	0.18	0.04	0.08	0.03	0.17	0.07	0.03	0.01
ratio mean within-ind. dist. to error	2.15****	2.58****	2.40****	2.99****	n/a	NaN	n/a	NaN	n/a	NaN
ratio mean between-ind. Dist. to error	3.77****	11.06****	4.10****	19.42****	14.47****	65.74****	12.53****	53.62****	23.61****	86.08****

22

23 **TABLE A1**

24

	FM	SS	SSD	EE	EED	PL	MD	MDD	SA	SAD	SI	SID	EL	ELD	PC1	PC2	PC3
Back legs																	
F (sides)	0.03	1.50	0.78	3.10	11**	40****	3.80	2.20	16***	2.10	7.4**	1.90	11**	1.80	9.4**	12***	3.1
F (individuals)	300****	35****	4.4****	51****	4.3****	25****	70****	20****	86****	19****	2e+02****	16****	23****	6.3****	150****	95****	160****
F (sides x individuals)	7.5****	12****	5.2****	30****	7.4****	15****	12****	3.8****	12****	4****	96****	5****	15****	5.1****	74****	53****	79****
p (mean left = mean right)	0.98	0.63	0.52	0.59	0.03	0.01	0.55	0.44	0.26	0.44	0.65	0.45	0.15	0.35	0.56	0.41	0.74
Front legs																	
F (sides)	0.86	3.20	2.00	1.30	1.20	4.2*	0.01	0.07	4.8*	1.70	67****	0.22	0.34	4*	53****	28****	52****
F (individuals)	350****	87****	57****	19****	3.9****	34****	24****	17****	170****	1.2e+02**	380****	9****	28****	16****	280****	160****	310****
F (sides x individuals)	9.7****	8.4****	20****	8****	6.2****	6.1****	2*	2.3*	13****	9.2****	4.6****	2.6**	5****	2.3*	5****	5.3****	3.9****
p (mean left = mean right)	0.89	0.61	0.65	0.57	0.43	0.38	0.96	0.88	0.64	0.75	0.23	0.75	0.79	0.24	0.22	0.24	0.24

25

26 **TABLE A2**

27

	PC1	PC2	PC3	PC4	PC5	PC6	PC7	PC8	PC9	PC10	PC11	PC12	PC13	PC14
FM	0.35	-0.18	0.03	-0.02	-0.03	-0.33	-0.10	0.13	-0.17	0.54	0.51	0.09	0.35	0.00
SS	0.37	0.14	-0.12	-0.16	0.10	0.10	-0.03	0.11	-0.22	0.19	-0.09	-0.16	-0.49	0.65
SSD	0.36	0.13	-0.11	0.03	0.04	0.26	0.21	0.02	0.41	-0.10	0.51	0.17	-0.41	-0.30
EE	0.18	0.13	0.55	-0.24	-0.10	0.20	-0.14	0.60	0.24	-0.07	-0.11	-0.21	0.17	-0.05
EED	0.06	-0.07	-0.52	0.57	-0.24	0.22	-0.25	0.45	0.01	-0.03	-0.08	-0.05	0.11	0.01
PL	-0.24	0.25	-0.31	-0.23	-0.17	-0.25	0.67	0.37	0.10	0.20	-0.10	0.01	0.05	0.00
MD	-0.13	0.50	-0.18	-0.27	-0.16	-0.07	-0.26	0.06	-0.39	-0.42	0.42	-0.06	0.09	-0.01
MDD	-0.18	0.49	-0.08	-0.06	-0.16	0.03	-0.42	-0.25	0.43	0.50	-0.09	0.04	-0.01	0.01
SA	0.34	0.13	-0.23	-0.21	0.20	0.15	-0.01	-0.08	-0.32	0.19	-0.34	-0.27	0.04	-0.61
SAD	0.35	0.16	-0.19	-0.11	0.17	0.26	0.17	-0.23	0.19	-0.20	-0.10	0.22	0.63	0.32
SI	-0.28	0.18	0.25	0.25	0.01	0.62	0.29	-0.07	-0.34	0.31	0.23	-0.08	0.11	0.05
SID	-0.18	0.25	-0.01	0.22	0.86	-0.17	-0.09	0.28	0.06	0.02	0.06	0.05	0.02	0.00
EL	0.24	0.36	0.28	0.29	-0.17	-0.17	0.05	0.05	-0.28	-0.02	-0.28	0.64	-0.11	-0.09
ELD	0.24	0.30	0.17	0.46	-0.10	-0.35	0.21	-0.23	0.11	-0.12	0.03	-0.59	0.07	0.04
Var. expl.	44.92	17.91	12.01	7.87	5.20	3.31	2.81	2.30	1.26	0.94	0.70	0.46	0.27	0.04
	'spot size'	wavelength'	spot shape'											

28

29 **TABLE A3**

30

	FM	SS	SSD	EE	EED	PL	MD	MDD	SA	SAD	SI	SID	EL	ELD
Left back leg	0.71	0.18	0.51	0.11	0.21	0.99	0.34	0.54	0.36	0.56	0.22	0.26	0.13	0.35
Right back leg	0.64	0.15	0.48	0.08	0.37	0.53	0.49	0.63	0.32	0.44	0.21	0.23	0.12	0.43
Left front leg	0.52	0.24	0.51	0.08	0.15	0.60	0.23	0.42	0.45	0.76	0.19	0.21	0.09	0.30
Right front leg	0.53	0.20	0.51	0.09	0.24	0.87	0.31	0.52	0.50	0.83	0.20	0.20	0.09	0.35
Head	0.13	0.25	0.31	0.06	0.18	0.20	0.19	0.28	0.50	0.49	0.20	0.23	0.13	0.28
Trunk	0.59	0.29	0.58	0.11	0.18	1.34	0.61	0.83	0.50	0.67	0.24	0.38	0.18	0.43
Tail	0.16	0.16	0.27	0.05	0.18	0.19	0.18	0.39	0.34	0.34	0.21	0.23	0.10	0.28
All body parts	0.56	0.34	0.67	0.09	0.21	1.20	0.44	0.69	0.66	0.87	0.30	0.32	0.17	0.48

31

32 **TABLE A4**

33